May 2017

Devices Selection and Topology Comparison for Medium Voltage DC Solid State Circuit Breakers

Yihui Zhang
University of Wisconsin-Milwaukee

DEVICES SELECTION AND TOPOLOGY COMPARISON FOR MEDIUM VOLTAGE DC SOLID STATE CIRCUIT BREAKERS

by

Yihui Zhang

A Thesis Submitted in

Partial Fulfillment of the

Requirements for the Degree of

Master of Science

in Engineering

at

The University of Wisconsin-Milwaukee

May 2017

ABSTRACT

DEVICES SELECTION AND TOPOLOGY COMPARISON FOR MEDIUM VOLTAGE DC SOLID STATE CIRCUIT BREAKERS

by

Yihui Zhang

The University of Wisconsin-Milwaukee, 2017
Under the Supervision of Professor Robert M. Cuzner

DC grid has been treated as a viable solution to solve green-house effect and reduce the cost of fossil fuels. Compared with AC grid, DC grid shows many inherent advantages, such as high efficiency power delivery, less expensive to deploy and no need for phase and frequency synchronization. However, over current protection for DC grid require fast response. To solve this problem, solid state DC circuit breakers need to be promoted.

In this thesis, thermal property was taken into consideration to find the most suitable semiconductor devices. Per unitized thermal resistance of the heat sink to the ambient was used to find the reasonable conducting current. Module MOV topology and one MOV topology were compared to see the voltage and current stress

ANSYS Simplorer is used to assist in the process. Simulation is used to see the waveform of the current stress and the voltage stress under ideal and non-ideal condition. According to the results, during the ideal condition the current stress and the voltage stress are almost the same. However, under the non-ideal condition, the current stress and voltage stress are different, and the module MOV mode topology is much more reliable and has less current and voltage stress.

TABLE OF CONTENTS

LIST OF FIGURES

LIST OF TABLES

LIST OF EQUATIONS

ACKNOWLEDGMENTS

Chapter 1 Introduction 1

1.1 Background 1

1.2 Research Status 3

1.2.1 System Specification 3
1.2.2 Requirement of DC Grid Protection 3
1.2.3 DC Solid State Circuit Breakers 4
1.2.4 Semiconductor devices 5
1.2.5 Voltage Sharing and Current Sharing Problems 10

1.3 Research Objective and Article Layout 15

1.3.1 Research Objective 15
1.3.2 Article Layout 16

Chapter 2 Device Selection 17

2.1 Thermal Resistance 17

2.1.1 Temperatures 18
2.1.2 Thermal Resistance 19
2.1.3 Thermal Equivalent Network 19

2.2 Calculation of conduction loss 20

2.3 Efficiency Calculation 23

2.4 Device Selection 24

Chapter 3 Metal Oxide Varistor 27

3.1 V/I Characteristic 27

3.2 Operation Voltage 29

3.3 Surge current, transient 29

3.4 Energy absorption 29

3.5 Equivalent circuits 30

Chapter 4 Simulation and Result 33
4.1 Modeling 33

4.2 Simulation model parameters 35

4.3 Result and Analysis.. 36

4.3.1 Ideal condition 36
4.3.2 Non-ideal condition 41
Chapter 5 Conclusion and Future Work.. 51
5.1 Conclusion 51

5.2 Future Work.. 51

References... 52

LIST OF FIGURES

Figure 1-1 The symbol of thyristor 5

Figure 1-2 The *i*-*v* characteristics of thyristor 5

Figure 1-3 The symbol of GTO 6

Figure 1-4 The *i*-*v* characteristics of GTO 7

Figure 1-5 The symbol of IGBT 8

Figure 1-6 The *i*-*v* characteristics of IGBT 8

Figure 1-7 The symbol of MOSFET 9

Figure 1-8 The *i*-*v* characteristics of MOSFET 9

Figure 1-9 Static and dynamic current sharing circuit topology 15

Figure 1-10 Resistor in series with the gate current sharing theory 15

Figure 2-1 Thermal resistance and equivalent thermal circuits 18

Figure 2-2 Modeling of the thermal interface 19

Figure 2-3 Thermal resistance equivalent circuit 20

Figure 2-4 IGBT output characteristic 22

Figure 3-1 Real V/I characteristic and ohmic resistance 28

Figure 3-2 Equivalent circuit 31

Figure 4-1 Module MOV mode simulation model 34

Figure 4-2 One MOV mode simulation model 35

Figure 4-3 The current and voltage of an IGBT module and the voltage of MOV under Module MOV mode faults occurs at 10m 36

Fig Figure 4-4 The dissipation energy of MOV under Module MOV mode faults occurs at 10m under ideal condition........ 38

Figure 4-5 The current and voltage of an IGBT module and the voltage of MOV under module MOV mode faults occurs at 300m........ 38

Figure 4-6 The dissipation energy of MOV under Module MOV mode faults occurs at 300m ideal condition........ 39

Figure 4-7 The current and voltage of an IGBT module and the voltage of MOV under one MOV mode faults occurs at 10m........ 39

Figure 4-8 The dissipation energy of MOV under one MOV mode faults occurs at 10m ideal condition........ 40

Figure 4-9 The current and voltage of an IGBT module and the voltage of MOV under one MOV mode faults occurs at 300m........ 40

Figure 4-10 The dissipation energy of MOV under one MOV mode faults occurs at 10m ideal condition........ 41

Figure 4-11 The gate signal of V1 is 2000ns earlier than others-current comparison of one MOV mode........ 42

Figure 4-12 The gate signal of V1 is 2000ns earlier than others-current comparison of module MOV mode........ 42

Figure 4-13 The gate signal of V1 is 2000ns earlier than others- currents through IGBT module MOV and paralleled inductance........ 43

Figure 4-14 The gate signal of V1 is 2000ns earlier than others-voltage comparison of one MOV mode........ 43

Figure 4-15 The gate signal of V1 is 2000ns earlier than others-voltage comparison of module MOV mode 44

Figure 4-16 The gate signal of V1 and V7 is 2000ns earlier than others-voltage comparison of module MOV mode 44

Figure 4-17 The gate signal of V1 and V7 is 2000ns earlier than others-voltage comparison of one MOV mode........ 45

Figure 4-18 The gate signal of V1 and V7 is 2000ns earlier than others- current comparison of one MOV mode........ 45

Figure 4-19 The gate signal of V1 and V7 is 2000ns earlier than others-current comparison of module MOV mode 46

Figure 4-20 The resistance of V1 and V7 is 0.1mΩ greater than others-voltage comparison of one MOV mode........ 46

Figure 4-21 The resistance of V1 and V7 is 0.1mΩ greater than others-voltage comparison of module MOV mode 47

Figure 4-22 The resistance of V1 and V7 is 0.1mΩ greater than others-current comparison of module MOV mode 47

Figure 4-23 The resistance of V1 and V7 is 0.1mΩ greater than others-current comparison of one MOV mode 48

Figure 4-24 The resistance of V1 and V7 is 0.1mΩ greater than others- urrent comparison of one MOV mode 48

Figure 4-25 The resistance of V1 and V7 is 0.1mΩ greater than others-current comparison of module MOV mode 49

Figure 4-26 The resistance of V1 and V7 is 0.1mΩ greater than others-voltage comparison of one MOV mode.. 49

Figure 4-27 The resistance of V1 and V7 is 0.1mΩ greater than others-voltage comparison of module MOV mode 50

LIST OF TABLES

Table 1 System Specification 3

Table 2 Component list.. 24

Table 3 Device parameters 24

Table 4 Calculation result.. 25

Table 5 Module MOV mode fault occurs at 300m.. 35

Table 6 Module MOV mode fault occurs at 10m.. 35

Table 7 One MOV mode fault occurs at 300m.. 35

Table 8 One MOV mode fault occurs at 10m.. 36

Table 9 different modes comparison 41

LIST OF EQUATIONS

Equation 2-1 19

Equation 2-2 20

Equation 2-3 21

Equation 2-4 21

Equation 2-5 21

Equation 2-6 22

Equation 2-7 24

Equation 3-1 27

Equation 3-2 27

Equation 3-3 28

Equation 3-4 28

Equation 3-5 28

Equation 3-6 29

ACKNOWLEDGEMENTS

First of all I would like to express my heartfelt gratitude to my advisor Professor Robert M. Cuzner for his patient guidance. I sincerely appreciate for all those discussions and conversations in which Professor Cuzner shared his invaluable knowledge and experience, and helped me to work out difficulties. I feel so lucky and blessed to have such a great advisor who spears no effort to help students. I would like to specifically thank Professor David C. Yu, for his support and encouragement to me, and for his effort to build up the cooperative relationship between University of Wisconsin-Milwaukee and the universities in China, which provide opportunities to students like me to study here.

Additionally, I want to thank my friends for their advice in my work and help in my life, especially thank Mengyuan Qi and Junyang Yu for their help both in my study and personal life.

Finally, I would like to express my deepest appreciation to my family, for their unconditional love and support, only with their love I can go so far to know more about the wonderful world.

Chapter 1 Introduction

In this chapter, the background, research status, and general approach are presented.

1.1 Background

With the rapid development of power system, modern power system is facing a series of new contradictions and problems, but it is also faced with unprecedented challenges. With the power system continuing to expand, the short circuit current level is rapidly increased. Because of the slow functioning speed, the difficulty of arc extinguishes, and the limitation of the capacity, the existing circuit breakers cannot meet the requirement of the increasing breaking capacity. In many situations, functioning speed is significant, especially about the power system stability control. For that reason, the way to limit and interrupt the fault current rapidly becomes more and more important. However, the functioning speed of traditional mechanical circuit breakers were limited by the mechanical inertia, this hindered the improvement of the functioning speed of mechanical circuit breakers severely, and impact the fault interruption and the stability of the grid control. In addition, the reliability and the life of mechanical circuit breakers also cannot meet the requirement of modern power system.

In high voltage and medium voltage field, there are only high voltage DC circuit breaker which can transfer or breaking load current of the high voltage DC circuit breaker [1]. There are some companies did the research of the circuit breakers which can interrupt short circuit fault current. The DC solid state circuit breakers are developed with the technique of power electronic devices. In 1990s, a solid state switches with thyristors appeared. After that, the appearing of fully controllable devices such as integrated gate commutated thyristor (IGCT), insulated gate bipolar transistor (IGBT), etc makes further development of DC solid state circuit breakers. At present, solid-state DC circuit breakers based on power electronic devices can be divided into hybrid DC circuit breakers and solid-state DC circuit breakers [2]. The hybrid DC circuit breaker consists of power electronic devices and mechanical switches in parallel. Although under the normal operate condition, there is almost no on state loss, the time delay of interrupting the fault current is still determined by the mechanical circuit breaker action time. For all solid-state DC circuit breakers, although breaking time is short, there are high expense, high on-state loss, limited capacity of single device and other shortcomings. The continuous development of semiconductor devices, the reduction of devices losses, and the improvement of capacity provide a good foundation for the development of DC solid state circuit breakers.

The system inductance of a DC grid is usually smaller than AC grid. When a short circuit fault occurs in the DC grid, the fault current is determined by system voltage and the remaining resistance [3]. The rise rate of the fault current is limited by system inductance and the current limit inductor. The resistance and the inductance is smaller than AC grid, which can improve the transmission efficiency and reduce the loss during transmission. However, this will make the rise rate of fault current in DC grid much faster than it in AC grid. For that reason, it is very necessary to develop a type of circuit breakers which can interrupt the fault current before it comes to the maximum value.

This thesis is aimed to develop medium voltage DC solid circuit breakers. Based on the existing power electronic devices. It is necessary to series and parallel semiconductors to achieve medium voltage DC solid circuit breakers.

1.2 Research Status

In this section, DC system will be briefly described; research status of the DC circuit breakers will be presented.

Compared with AC transmission or distribution grid, DC transmission of distribution grid has lower loss of the cable, and there is no synchronization operation issue and a series advantages.

Solid state circuit breaker is a type of breakers which consist of fully controllable semiconductor in the current path.

1.2.1 System Specification

Table 1 System Specification

ratings	values
Voltage rating	20kV
Current rating	2000A
System capacity rating	40MVA

1.2.2 Requirement of DC Grid Protection

In reference [4], it talks about the requirement of the DC protection. The function for a protection system is to protect of the system itself and its user against damage while provide a reliable supply [4]. A power system protection scheme, regardless of AC or DC, should provide the properties or criteria listed in [5]. The criteria in particular concerning DC breakers are:

(1) Selectivity States the demand for DC circuit breakers in general, the protection system must be able to isolate faulted parts of the system only.

(2) Speed States the demand for the DC circuit breaker to operate before the fault current damages the power system and its users.

(3) Reliability States the requirement for the DC circuit breakers in the system to be able to conduct its required function under different modes and scenarios that may occur in DC grid [6].

The speed criterion provides some challenges due to fast rising fault currents seen in last section and in the introduction. The fault currents in DC grid may rapidly damage the free-wheeling diodes of the converter stations and thus the DC breaker should operate before the event of diode damage is likely to occur. As stated in the introduction, the protection system must clear the fault within a few ms [7].

1.2.3 DC Solid State Circuit Breakers

The solid state circuit breakers consist of semiconductor devices such as the insulated gate bipolar transistor (IGBT) or gate turn-off thyristor (GTO) and parallel MOVs. Some may have a parallel resistor and capacitance as a clamping circuit. The main difference between solid state circuit breakers and other kind of circuit breakers such as mechanical or hybrid circuit breakers is that solid state circuit breakers do not have a mechanical switch. Under normal condition, the load current flows through the power electronic devices branches. During normal operation condition, the power electronic devices are on. When faults occurs, to interrupt the fault current, the power electronic devices are switched off to commutate the fault current to parallel MOV branch. The functions of MOV are as the commutation and the energy absorbing path and clamp the voltage across the power electronic devices. Solid state circuit breakers can achieve to interrupt one directional and bi-directional fault current. Bi-directional circuit breakers can be achieved by anti-series two IGBTs with an anti-paralleled diode. By placing more power electronic modules in series to achieve higher rated voltage level, and placing more modules in parallel to increase the rated current level. The solid state circuit breaker has proven to break current with the required speed for fault current interruption. But as the semiconductors are conducting current under normal operating conditions, the losses due to the voltage drop over the breaker will be high especially in high voltage applications. This will also bring a challenge on thermal design.

1.2.4 Semiconductor devices

(1) Thyristor

The circuit symbol for the thyristor and its *i-v* characteristic are shown in Figure 1-1 and Figure 1-2. The main current flows from the anode (A) to the cathode (K). In its off-state, the thyristor can block a forward polarity voltage and not conduct by the off-state portion of the i-v characteristic. The forward voltage drop in the on state is only a few volts (typically 1-3 V depending on the device blocking voltage rating).

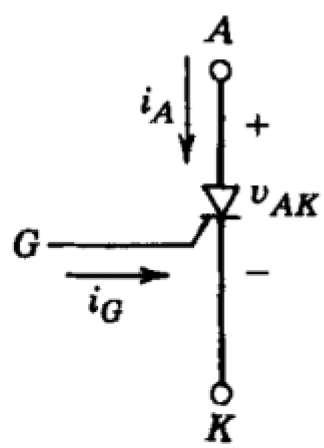

Figure 1-1 The symbol of thyristor

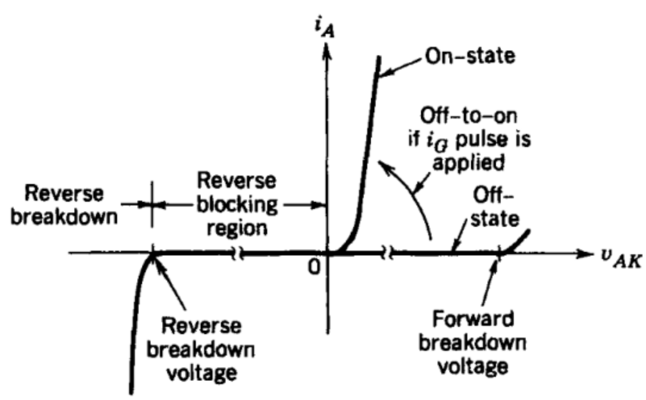

Figure 1-2 The *i-v* characteristics of thyristor

Once the device begins to conduct, it is latched on and the gate current can be removed. The thyristor cannot be turned off by the gate, and the thyristor conducts as a diode. Only when the anode current tries to go negative, under the influence of the circuit in which the thyristor is connected, does the thyristor turn off and the current go to zero. This allows the gate to regain control in order to turn the device on at some controllable time after it has again entered the forward-blocking state.

In reverse bias at voltages below the reverse breakdown voltage, only a negligibly small leakage current flows in the thyristor. Usually the thyristor voltage ratings for forward- and reverse-blocking voltages are the same. The thyristor current ratings are specified in terms of maximum rms and average currents that it is capable of conducting.

(2) Gate-Turn-Off Thyristor (GTO)

The circuit symbol for the GTO is shown in Figure 1-3 and its steady-state *i*-*v* characteristic is shown in Figure 1-4.

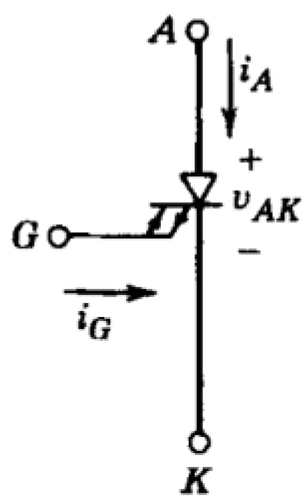

Figure 1-3 The symbol of GTO

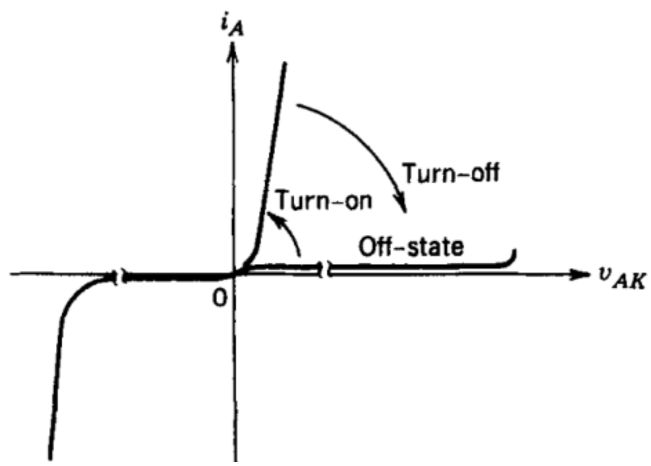

Figure 1-4 The *i-v* characteristics of GTO

Like the thyristor, the GTO can be turned on by a short-duration gate current pulse, and once in the on-state, the GTO may stay on without any further gate current. However, unlike the thyristor, the GTO can be turned off by applying a negative gate-cathode voltage, therefore causing a sufficiently large negative gate current to flow. This negative gate current need only flow for a few microseconds (during the turn-off time), but it must have a very large magnitude, typically as large as one-third the anode current being turned off. The GTOs can block negative voltages whose magnitude depends on the details of the GTO design.

The on-state voltage (2-3 V) of a GTO is slightly higher than those of thyristors. The GTO switching speeds are in the range of a few microseconds to 25 μs. Because of their capability to handle large voltages (up to 4.5 kV) and large currents (up to a few kilo amperes), the GTO is used when a switch is needed for high voltages and large currents in a switching frequency range of a few hundred hertz to 10 kHz.

(3) Insulated Gate Bipolar Transistor (IGBT)

The circuit symbol for an IGBT and its *i-v* characteristic are shown in Figure 1-5 and Figure 1-6. The IGBTs have some of the advantages of the MOSFET, the BJT, and the GTO combined. Similar to the MOSFET, the IGBT has a high impedance gate, which requires only a small amount of energy to switch the device. Like the BJT, the IGBT has a small on-state voltage even in devices with large blocking voltage ratings (for example, V_{on} is 2-3 V in a 1000V device). Similar to the GTO, IGBTs can be designed to block negative voltages.

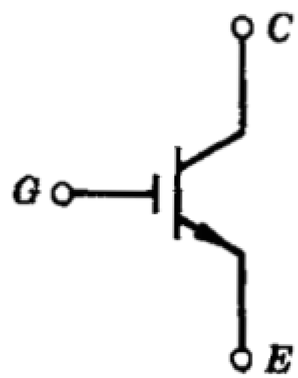

Figure 1-5 The symbol of IGBT

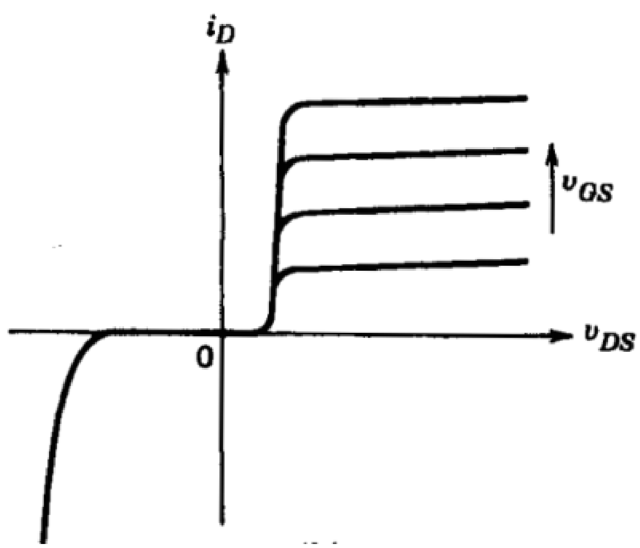

Figure 1-6 The *i-v* characteristics of IGBT

Insulated gate bipolar transistors have turn-on and turn-off times on the order of 1 μs and are available in module ratings as large as 1700 V and 1200A. Voltage ratings of up to 2-3 kV are projected.

(4) Metal- Oxide- Semiconductor Field Effect Transistor (MOSFET)

The circuit symbol of an n-channel MOSFET is shown in Figure 1-7. It is a voltage controlled device, as is indicated by the C v characteristics shown in Figure 1-8. The device is fully on and approximates a closed switch when the gate-source voltage is below the threshold value, $V_{GS(th)}$.

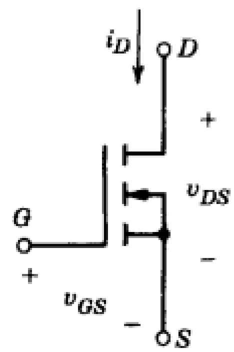

Figure 1-7 The symbol of MOSFET

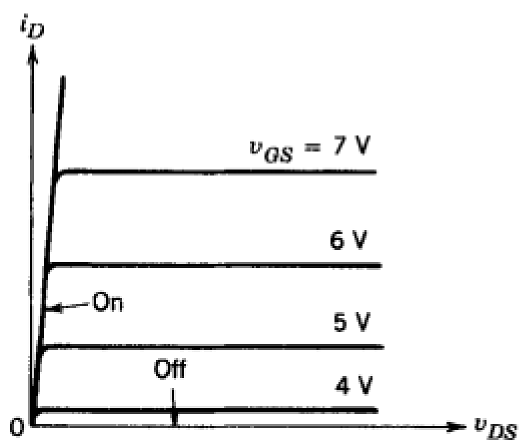

Figure 1-8 The *i-v* characteristics of MOSFET

Metal- oxide- semiconductor field effect transistors require the continuous application of a gate-source voltage of appropriate magnitude in order to be in the on state. No gate current flows except during the transitions from on to off or vice versa when the gate capacitance is being charged or discharged. The switching times are very short, being in the range of a few tens of nanoseconds to a few hundred nanoseconds depending on the device type.

MOSFETs are available in voltage ratings in excess of lo00 V but with small current ratings and with up to 100 A at small voltage ratings. The maximum gate-source voltage is 220 V, although MOSFETs that can be controlled by 5V signals are available.

Because their on-state resistance has a positive temperature coefficient, MOSFETs are easily paralleled. This causes the device conducting the higher current to heat up and thus forces it to equitably share its current with the other MOSFETs in parallel.

1.2.5 Voltage Sharing and Current Sharing Problems

(1) Cause Analysis of Series Voltage Sharing Problem

IGBT as the representative of the full control of switching devices, there are four working conditions: stable positive blocking state, stable conduction state, turn on the transient and turn off the transient. The first two states are static processes, and the turn-on and turn-off transients are dynamic processes. So the pressure in series can be divided into static pressure and dynamic pressure of two cases.

Static pressure is mainly for the positive stability of the block state of work, because in the steady state, the series switching devices conduction saturation voltage drop is about the same, around 1-3V, as long as there is no over current situation, the switch can work properly[8]. And for the positive stability of the block state, the device's forward volt-ampere characteristics may bring uneven voltage on the IGBT, which may lead to damage to the device. In the blocking state, the IGBT whose blocking impedance is lower, the turn off leakage current is larger will hold lower voltage than the IGBT whose blocking impedance is higher, turn off leakage current is smaller. So in the series structure, the most vulnerable device is the one which has the highest block. It is necessary to take the appropriate static pressure control strategy to protect from damage.

Dynamic pressure is mainly reflected in the moment of turning on and turning off [9]. Due to the impact of power electronic devices dynamic parameters, such as threshold voltage, input capacitance, Miller capacitance and gate resistance, gate drive voltage waveform and timing factors, inconsistent turn-on and turn-off times, resulting in a significant imbalance in the instantaneous voltage. First, the distribution parameters are closely related to the rate of dU/dt of the device during turning on and turning off, and different distribution parameters between the devices will result in inconsistencies in turn-on and turn-off, and my cause uneven dynamic voltage distribution. Second, the drive resistance parameters of gate drive circuit will also affect the dynamic pressure. The gate resistance in the turning on moment will produce voltage spikes, and the IGBT which has smaller gate resistance in the turning off period will have fast voltage rise rate. In addition, the gate trigger signal is not synchronized in time will bring the phenomenon of dynamic non-uniform pressure, which gate signal is turned on the device will appear when the voltage spikes, early shutdown of the device will also appear on the voltage spike, causing the dynamic voltage distribution of the series devices not even.

(2) Series Voltage Sharing Strategy

The prerequisite for the equalization of power electronic devices is to choose the devices with the same characteristic parameters as the best choice in the selection of the devices. At the same time, the circuit topology is optimized to make the circuit structure as symmetrical as possible. The driving circuit is kept consistent and the reasonable layout is ensured. The static voltage sharing problem in series is to parallel snubber resistor between the collector and the emitter of each series device to achieve static pressure equalization [10]. There are three main categories of dynamic pressure equalization strategy: parallel passive snubber circuit pressure strategy, the gate active control pressure control strategy and voltage clamp equalization strategy. Because of its simple structure, safe and reliable, parallel passive snubber circuit pressure control strategy is currently the most commonly used. It is often used resistor and capacitor snubber circuit to limit the collector voltage rise rate to make the voltage rise rate of each device is the same as the slowest device, so as to realize the purpose of dynamic pressure equalization. But the snubber circuit in the high-voltage lines will bring higher losses, and will reduce the device speed and switching frequency [11]. In reality, in the application, the size of the snubber circuit is relatively large, and the cost is higher.

(3) Cause Analysis of Parallel Current Sharing Problem

In order to improve the flow capacity of the DC circuit breaker, the all solid and hybrid circuit breakers need to parallel switching devices to ensure that the capacity is big enough to interrupt the short circuit current. But this brings the parallel current sharing problem of the switching devices. As with the series pressure, the parallel current sharing problem can be divided into static parallel current sharing and dynamic parallel sharing cases.

The reason for the static current sharing is related to the static characteristics of the switching devices. For the same type of IGBT, the voltage drop due to the saturation voltage drop of the device will result in the unbalanced voltage, and the device which has lower saturation voltage drop will withstand the greater shunt current, and easier to be damaged. For that reason, it is necessary to take appropriate static current sharing strategy to protect the IGBT.

Dynamic current sharing is mainly reflected in the different devices are not consistent with the instantaneous current in the moment of turning on and turning off. There are two main factors: one is the influence of the parameters of the device itself, the threshold voltage, gate capacitance, Miller capacitance is the main influencing factor. The second is the gate trigger circuit and the main circuit part, mainly related to gate resistance, gate lead inductance and emitter inductance circuit parameters of the impact. These factors cause the parallel disconnection time is not uniform. The IGBT whose turning on time is faster will bear a larger instantaneous current, and in turn off period, the one whose turning off speed is slower will bear a larger instantaneous current.

(4) Parallel Current Sharing Strategy

To achieve IGBT parallel current sharing, firstly, it is necessary to select the devices whose characteristics parameters are more consistent. Meanwhile, the circuit topology optimization is necessary, so that the circuit structures are more symmetrical. Reasonable layout can reduce the factors of the parallel current sharing problem. Under normal condition, compared to series voltage sharing problem, the parallel current sharing problem is not as severe as voltage sharing problem, so the research of parallel current sharing problem is not as popular as voltage sharing problem is. However, in practical application, it is very difficult to achieve complete parallel current sharing; for example, it is difficult to ensure the layout of the electrical circuit symmetrical perfectly, so that the distribution of the inductance has no impact on current sharing problem. It is also difficult to ensure the consistent of the drive signal. For that reason, It is still need to take some measures to improve the various factors that may lead to parallel current sharing problems.

The strategy of static current sharing is series the current sharing resistor of each branch in the parallel branch to achieve, as shown in Figure 1-9. If the value of sharing current resistor is much larger than the on state resistor, it can achieve the basic static current sharing balance.

The most common method of dynamic current sharing strategy is to achieve current sharing by using current sharing transformer. As shown in the Figure 1-9, the dynamic current sharing device can realize dynamic current sharing. In addition, the dynamic current sharing strategy also focus a lot on the use of gate control strategy of the current sharing scheme and gate drive circuit to achieve parallel IGBT current sharing program. Hofer et al. used the gate signal delay control method, through the closed-loop detection and control circuit makes the gate drive signal to maintain the consistency of time in order to achieve the parallel flow of IGBT parallel, this method in series dynamic pressure also used[11]. Chen et al. proposed a dynamic gate control method based on an average current that dynamically adjusts the IGBT drive voltage to achieve current sharing by detecting the current values and the average value [12]. By improving the gate structure, string into the gate compensation resistor can also be achieved by the dynamic current sharing, the basic structure shown in the Figure 1-10.

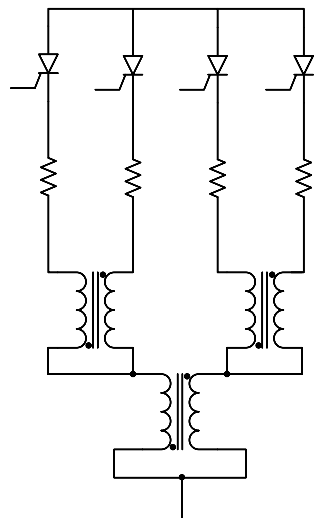

Figure 1-9 Static and dynamic current sharing circuit topology

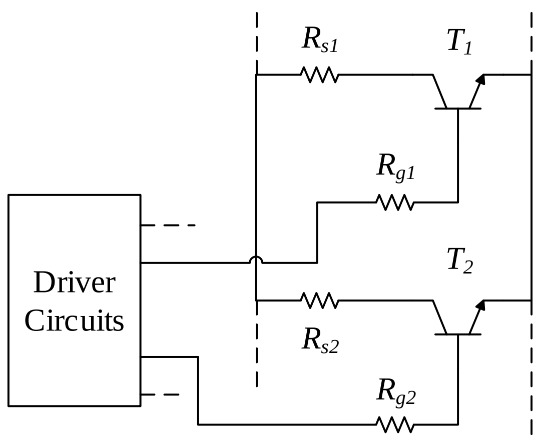

Figure 1-10 Resistor in series with the gate current sharing theory

1.3 Research Objective and Article Layout

1.3.1 Research Objective

The main research objective of this thesis is to select a most suitable semiconductor device to meet the 2000A high rating current and 20kV medium level rating voltage. The requirement of medium voltage DC solid state circuit breakers need to meet the high voltage rating which need to series some semiconductors together, and need to meet the high current rating which need to have some parallel branches to improve the current capacity. Because of the semiconductor branches are the current path during normal operation condition, the high conduction loss is the shortcoming of the solid state circuit breakers. Meanwhile, the high conduction loss will make cooling system more complex. For that reason, we take thermal property into consideration to find the proper conducting current of every device.

MOV is treated as an energy dissipation device and can protect semiconductors from the damage of over voltage. We compared two mode of the MOV topology. Because different connection ways may have different stray inductance distribution, then makes the current stress and voltage stress have different value. Finally, we figure out the influence caused by drive signal unsynchronized and manufacture difference.

1.3.2 Article Layout

The layout of this article is:

Device selection-considering thermal property and efficiency

Current and voltage sharing problem-the reason and the strategy to prevent it

Different MOV topology comparison-current stress and voltage stress

Chapter 2 Device Selection

Because this thesis is aimed at a medium voltage DC solid state circuit breakers, one thing need to be taken into consideration is its on state loss. For the devices need to be selected, the nominal voltage of each device is kilo volts level, and has an on-state voltage drop in the order of some volts. This means constant losses in the kilowatt range when conducting some hundred amperes. Every device has a nominal operation temperature, usually the maximum temperature is no more than 150℃. Because the resistance is proportional to the temperature, to achieve lower on state loss, it is important to keep the devices under a reasonable temperature. What is more, when the short circuit fault occurs, the switches need to interrupt the fault current. Due to its large value, there must be a large amount of heat generated by the semiconductors, so it is very necessary to take into thermal properties into consideration to keep safe and efficiency operation. A violation of the temperature ratings can lead to a reduced safe operating area and consequently a sudden device failure or to a reduced operational lifetime. If the thermal property of the semiconductors can hardly meet the requirement, this will require a large and complex cooling system.

2.1 Thermal Resistance

Thermal resistance is a heat property and a measurement of a temperature difference by which an object or material resists a heat flow.each part has a thermal resistance.

For an IGBT package as shown in Figure 2-1. It has junctions, case and heat sink. The heat flow goes through the junction

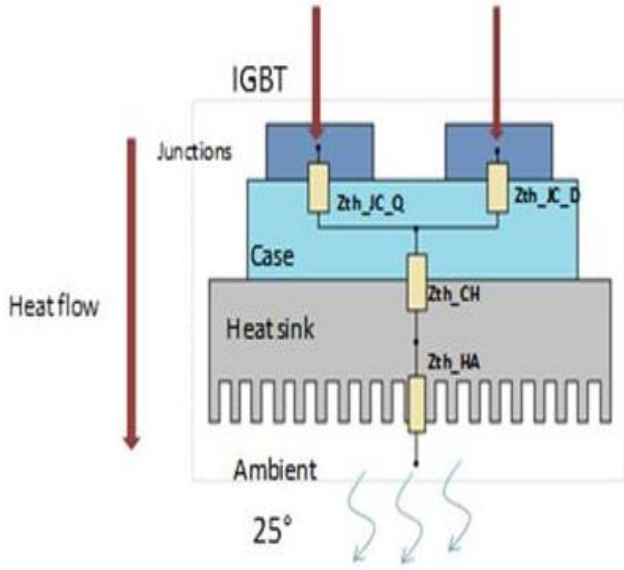

Figure 2-1 Thermal resistance and equivalent thermal circuits

2.1.1 Temperatures

Junction temperature: the junction temperature describes the temperature inside the chip which is relevant for the losses and safe operating area. $T_{vj,max}$ describes the maximum allowed dynamic junction temperature in the device on-state. Even under dynamic overload the device is not allowed to exceed the $T_{vj,max}$ value in on-state[13].

The case temperature (T_c) defines the allowed temperature range of the module case in operation. The case temperature range can differ from virtual junction temperature range. For instance the maximum case temperature can be lower than $T_{vj,opmax}$. This is because the plastic materials used for power modules cases have temperature limits. This though usually does not restrict operation in application conditions since there is always a temperature gradient from junction to case and devices operated with T_{vj}= 150 °C usually have a case temperature of less than 125 °C [13].

Heat sink temperature T_h: The heat sink temperature describes the surface temperature of the heat sink/cooler on which the power-module is mounted.

Ambient temperature: Ta it is the temperature around the environment. Usually it is assumed at 25℃.

2.1.2 Thermal Resistance

In newer datasheets thermal interface resistance (Rth(c-h)) is usually stated separately for IGBT and Diode. This is a more realistic simplification if the cross-talk between IGBT and Diode is considered which shown in Figure 2-2. Nevertheless if for some reason Rth(c-h) for the full module is needed, but the datasheet specifies it separately for IGBT and Diode, a simple parallel connection can be done using Equation 2-1[13]:

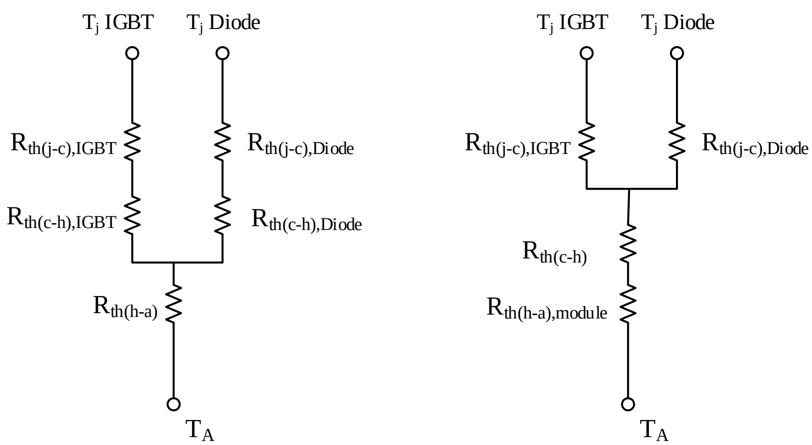

Figure 2-2 Modeling of the thermal interface

$$R_{th(c-h),\mathrm{module}} = \frac{R_{th(c-h),IGBT} \cdot R_{th(c-h),Diode}}{R_{th(c-h),IGBT} + R_{th(c-h),Diode}} \qquad \text{Equation 2-1}$$

2.1.3 Thermal Equivalent Network

The heat flow can be modeled by analogy to an electrical circuit where heat flow is represented by current, temperatures are represented by voltages, heat sources are represented by constant current sources, and absolute thermal resistances are represented by resistors and thermal capacitances by capacitors, as shown in Figure 2-3.

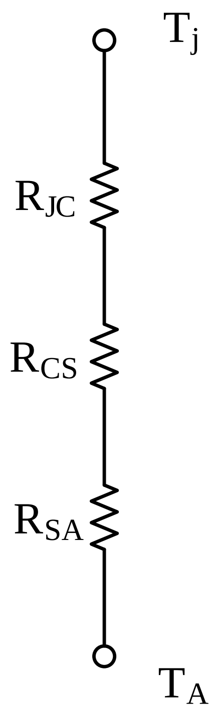

Figure 2-3 Thermal resistance equivalent circuit

2.2 Calculation of conduction loss

The power loss of an IGBT is made up with steady state conduction loss and switch loss. The switching loss of the IGBT consists switch on loss and switch off loss. The anti-paralleled diode has the conduction loss and reverse recovery loss. The total loss of an IGBT is summed up these losses together. In an IGBT module there are many IGBT die and diode die depending on the module and requirements of the application. All chips dissipate power when they are conducting or switching from one state to another [14].

During most of the time, the state of the solid state circuit breaker keeps turning on, and it seldom turns on or turns off, so the dominant loss of this situation is conduction loss. The following part will introduce the way to calculate the conduction loss. We take IGBT as an example, and the conduction loss of other semiconductors are almost the same, and the difference will be pointed out separately.

The conduction losses are on-state losses of steady state losses are the losses which appear during the IGBT and freewheeling diode is on and there is current flowing through them. The total power dissipation during conduction is calculated by multiplying the on-state current (Ic) and the on-state voltage (Vce).

The average conduction loss by IGBT is calculated by the following equation:

$$V_{CEsat} = \mathrm{V}_{\mathrm{TO}} + R_T \times I_C \qquad \text{Equation 2-2}$$

$$P_{cond} = V_{CEsat} \times I_c \qquad \text{Equation 2-3}$$

$$R_T = \frac{\Delta V}{\Delta I} = \frac{V_{CE2} - V_{CE1}}{\mathrm{I}_{C2} - \mathrm{I}_{C1}} \qquad \text{Equation 2-4}$$

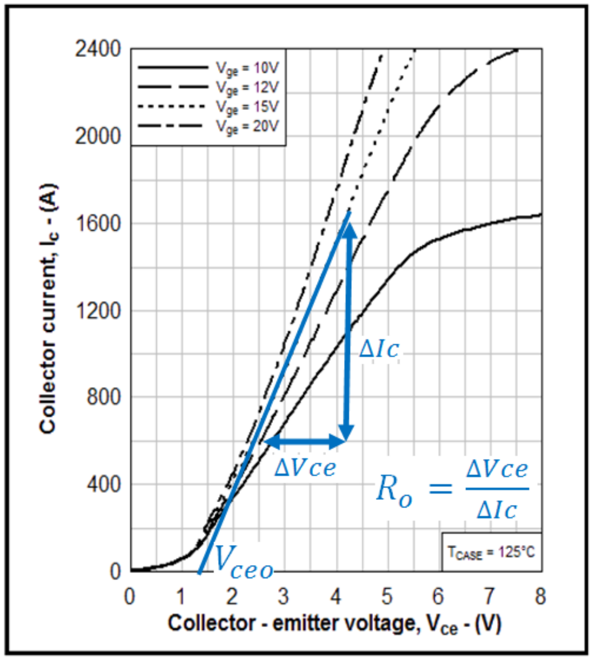

Figure 2-4 IGBT output characteristic

The value for R_T resistance can be easily calculated from the IGBT output characteristic curve from the datasheet. From Figure 2-4 we can linear the output characteristic curve around a very little fraction of the curve to get the resistance value. V_{TO} is the threshold voltage which can get from the datasheet. For MOSFET, the value of V_{TO} is zero.

After we get the value of conduction loss, we can start calculating the value of the thermal resistance between the heat sink and the ambient.

The value of the thermal resistance Rsa can be easily get from the following equation:

$$\frac{T_{j\max} - T_A}{P_{cond}} = R_{SA} + R_{JC} + R_{CS} \quad \text{Equation 2-5}$$

The value of T_{jmax}, R_{jc} and R_{cs} can be got from the date sheet, and Pcond can be calculated from equation 2-4. After we get the value of R_{SA} we should per unitize it to check the thermal property of this condition. As the thermal resistance is inversely proportional to area, to find the thermal resistance of a certain area cold plate, we should multiply the area (in square inch) of the cold plate.

The purpose of calculating the R_{SA} is that it is a value to show whether the certain conduction loss caused by a certain value of a current can meet the requirement of the thermal property. When the conducting current is so big, it will cause the cooling system cannot cool the heat through the device. This will lead to devices overheated which may damage the performance of the semiconductors and reduce the lifetime of devices.

From the [15] we can know that the reasonable value of R_{SA} is around 0.1-0.2 in per unitize. The lower the value the higher requirement of the cold plate. If the value of RSA is lower than 0.1 this means the big pressure for the cold plate. This will cause the cold plate thicker of the cooling water runs much faster, which is not reality. So when the value of RSA smaller than 0.1, Ic should be decreased. The existing cooling system cannot meet the thermal requirement or cool the heat which generated by that current value. The strategy of finding the proper conducting current value is:

If it is less than 0.1, reduce the current value

If it is greater than 0.1, increase the current value

2.3 Efficiency Calculation

From the literature [16] we know that parallel semiconductors can increase the efficiency of the circuit breakers, so after meet the requirement of the thermal requirement, the efficiency of the devices also need to be taken into consideration. Because the rating system capacity is 40MW, the efficiency should be high enough to reduce the conduction loss. The efficiency should greater than 99.99, even that the value of the conduction loss is still not a little number. In order to achieve that, we can lower the current of every single semiconductor and parallel more modules. The efficiency of the circuit breaker is given as,

$$\text{Efficiency}= \frac{40\text{MW}}{\text{total loss}+40\text{MW}} \quad \text{Equation 2-6}$$

2.4 Device Selection

After the basic knowledge of thermal property and the efficiency calculation we can use the methods above to select proper devices. Things need to be taken into consideration when select semiconductor for medium voltage DC solid state circuit breakers are rating voltage, rating current, thermal properties, efficiency and the number of the devices.

Table 2 is the devices we choose from.

Table 2 Component list

Manufacturer	**Specifications**
Infineon IGBT [17]	6.5kV 600A
Infineon IGBT [18]	6.5kV 750A
ABB IGBT [19]	6.5kV 600A
ABB IGBT [20]	6.5kV 750A
ABB GTO [21]	4.5kV 210A
ABB Thyristor [22]	3kV
ABB Thyristor [23]	2.4kV

Table 3 is the necessary parameters of each device according from the datasheet.

Table 3 Device parameters

Parameters / Types	Vrate/kV	Vto/kV	Ic/A	Rt/Ω	Pcon/kW	Tjmax/℃	Ta/℃	Rjc/K/kW	Rcs/K/kW	Area/inch^2
Infineon IGBT 6.5kV 600A	3.6	1	600	0.003	1.9175	125	25	10.2	9.2	41.22992
Infineon IGBT 6.5kV	3.6	1	750	0.0026	1.974	125	25	8.7	8.8	41.22992

750A										
ABB IGBT 6.5kV 600A	3.6	1.8	600	0.0043	2.628	125	25	11	6	41.22992
ABB IGBT 6.5kV 750A	3.6	1.25	750	0.003	2.625	125	25	11	9	41.22992
ABB Thyristor 2.4kV	1.6	2.045	617	0.000365	1.40071649	125	25	32	10	4.17
ABB Thyristor 3kV	2	2.149	1112	0.000258	2.70871635	125	25	16	4	6.75
ABB Thyristor 3kV	2	2.562	1003	0.000246	2.81716421	125	25	16	4	6.75
ABB GTO 4.5kV	4.5	1.9	200	0.0035	0.52	125	25	11.4	8	4,52

Table4 is the result of the thermal property calculation.

Table 4 Calculation result

Parameters / Types	RsaK/kW	p.u./K/W.inch^2	series	parallel	module	total
Infineon IGBT 6.5kV 600A	13.3746	0.175717	6	4	2	12
Infineon IGBT 6.5kV 750A	9.23258	0.160329	6	3	1	6
ABB IGBT 6.5kV 600A	7.01725	0.14466	6	5	2	12
ABB IGBT 6.5kV 750A	6.031746	0.124344	6	4	2	12
ABB Thyristor 2.4kV	29.39203	0.122565	9	2		18
ABB Thyristor 3kV	16.91786	0.114196	7	3		21
ABB Thyristor 3kV	15.49669	0.104603	7	3		21
ABB GTO 4.5kV 210A	44.70256	0.202056	5	10		50

According to the calculation result we can see that IGBT is the most suitable devices considering the thermal property and the number of the semiconductor. After thermal calculation we need to do the efficiency calculation, and the efficiency should greater than 99.99. In order to achieve that, we can lower the current of every single IGBT and parallel more modules.

After calculation, *Infineon 6.5kV 750A* is the most suitable device. The number of device is 6 modules in series, 2 branches in parallel, which makes its total number 12.

Chapter 3 Metal Oxide Varistor

The Metal Oxide Varistor (MOV) is a non-linear resistor. The MOV is traditionally used as overvoltage protection in power systems [24], [25], but their characteristics make them suitable as energy absorbing elements in breakers. The V–I characteristics of the MOV can be divided into two regions separated by a steep rise in the voltage.

Varistors (variable resistors) are voltage-dependent resistors with a symmetrical V/I characteristic curve whose resistance decreases with increasing voltage. Connected in parallel with the electronic device or circuit that is to be guarded, they form a low-resistance shunt when voltage increases and thus prevent any further rise in the surge overvoltage.

3.1 V/I Characteristic

The voltage dependence of varistors or VDRs (voltage dependent resistors) may be approximately characterized by the formula [26]

$$I = K \cdot V^{\propto} \qquad \text{Equation 3-1}$$

where, I: Current through varistor

K: Ceramic constant (depending on varistor type)

V: Voltage across varistor

α: Nonlinearity exponent

Another possible interpretation of the physical principle underlying these curves is that of a voltage-dependent resistance value, and particularly its rapid change at a predetermined voltage.

$$R = \frac{V}{I} = \frac{V}{KV^{\alpha}} = \frac{1}{K}V^{1-\alpha} \qquad \text{Equation 3-2}$$

Equations 3-3 and 3-4 can be shown particularly clearly on a log-log scale, because power functions then appear as straight lines:

$$\log I = \log K + \alpha \log V \qquad \text{Equation 3-3}$$

$$\log R = \log\left(\frac{1}{K}\right) + (1 - \alpha)\log V \qquad \text{Equation 3-4}$$

Determine the nonlinearity exponent α

Two pairs of voltage/current values (V_1/I_1 and V_2/I_2) are read from the V/I characteristic of the varistor and inserted into equation 3-5, solved for α:

$$\alpha = \frac{\log I_2 - \log I_1}{\log V_2 - \log V_1} \qquad \text{Equation 3-5}$$

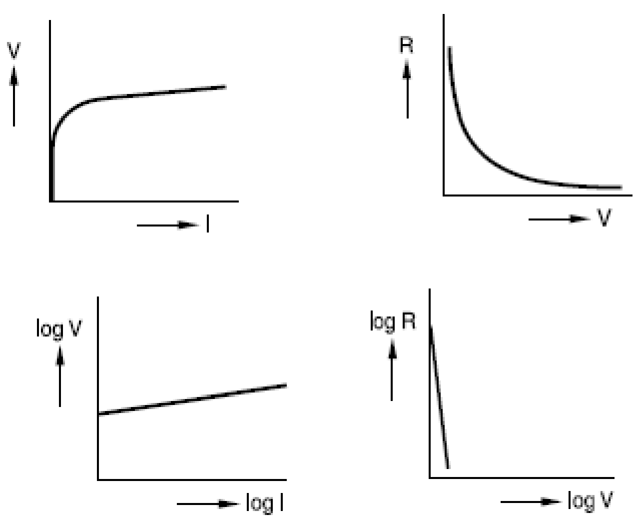

Figure 3-1 Real V/I characteristic and ohmic resistance

Normally α is determined according to equation 3-5 from the pairs of values for 1A and 1 mA of the V/I characteristic.

Where α means the “nonlinearity” exponent and in this way may be interpreted as a measure of the “steepness” of the V/I characteristic. In metal oxide varistors it has been possible to produce α figures of more than 30. Exceptional current handling capability combined with response times of less than 25 ns make them an almost perfect protective device.

3.2 Operation Voltage

The product tables specify maximum AC and DC operating voltages. These figures should only be exceeded by transients. Automotive types, however, are rated to withstand excessive voltage (jump start) for up to 5 minutes. The leakage current at specified operating voltage is negligible. The maximum permissible AC operating voltage is used to classify the individual voltage ratings within the type series. In most applications the operating voltage is a given parameter, so the varistors in the product tables are arranged according to maximum permissible operating voltage to facilitate comparison between the individual varistor sizes [28].

3.3 Surge current, transient

Short-term current flow–especially when caused by overvoltage–is referred to as surge current or transient.

The maximum surge current that can be handled by a metal oxide varistor depends on amplitude, pulse duration and number of pulses applied over device lifetime. The ability of a varistor to withstand a single pulse of defined shape is characterized by the maximum non-repetitive surge current specified in the product tables (single pulse, t_r <20 μs).

The maximum non-repetitive surge current is defined by an 8/20 ms waveform (rise time 8 ms/ decay time to half value 20 ms) according to IEC 60060 as shown in Figure 16. This waveform approximates a rectangular wave of 20 µs. The derating curves of the surge current, defined for rectangular waveforms, consequently show a knee between horizontal branch and slope at 20 µs [29].

3.4 Energy absorption

The energy absorption of a varistor is correlated with the surge current by

$$W = \int_{t_0}^{t_1} v(t)i(t)dt \qquad \text{Equation 3-6}$$

where v(t) is the voltage drop across the varistor during current flow.

3.5 Equivalent circuits

Figure 3-2(a) shows the simplified equivalent circuit of a metal oxide varistor. From this the behavior of the varistor can be interpreted for different current ranges [30].

Leakage current region ($<10^{-4}$ A)

In the leakage current region the resistance of an ideal varistor goes towards, so it can be ignored as the resistance of the intergranular boundary will predominate. Therefore $R_B << R_{IG}$. This produces the equivalent circuit in Figure 3-2(b):

The ohmic resistance R_{IG} determines behavior at low currents, the V/I curve goes from exponential to linear (downturn region).

R_{IG} shows distinct temperature dependence, so a marked increase in leakage current must be expected as temperature increases.

Normal operating region ($10^{-5}$to 10^{3}A)

With $R_V<<R_{IG}$ and $R_B << R_V$, R_V determines the electrical behavior (Figure 3-2(c)). The V/I curve (Figure 3-1) follows to a good approximation the simple mathematical description by an exponential function (equation 3-3) where $\alpha> 30$, i.e. the curve appears more or less as a straight line on a log-log scale.

High-current region (> 103 A)

Here the resistance of the ideal varistor approaches zero. This means that $R_V<<R_{IG}$ and $R_V < R_B$ (Figure 3-2(d)). The ohmic bulk resistance of ZnO causes the V/I curve to resume a linear characteristic (upturn region).

Capacitance

Equivalent circuits 3-2(a) and 3-2(b) indicate the capacitance of metal oxide varistors (see product specifications for typical values). In terms of overvoltage suppression, a high capacitance is desirable because, with its low pass characteristic, it smoothes steep surge voltage edges and consequently improves the protection level.

Lead inductance

The response time of the actual varistor ceramics is in the picoseconds region. In the case of leaded varistors, the inductance of the connecting leads causes the response time to increase to values of several nanoseconds. For this reason, all attempts must be made to achieve a mounting method with the lowest possible inductance i.e. shortest possible leads.

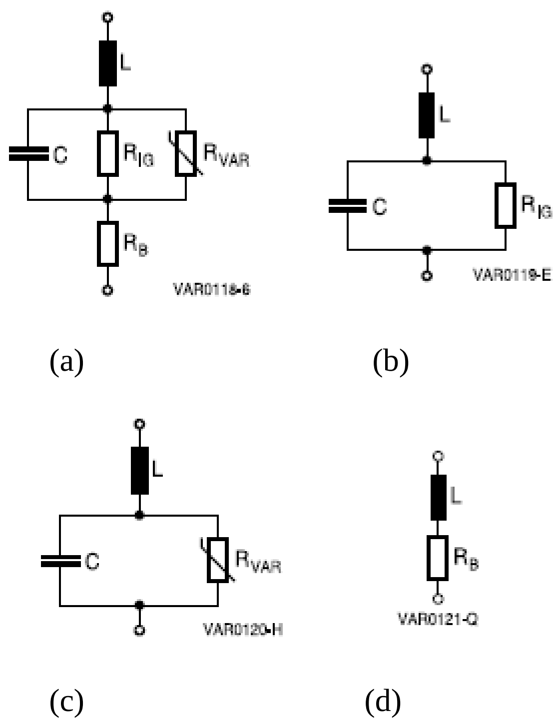

Figure 3-2 Equivalent circuit

L: Lead inductance (≈1 nH/mm)

C: Capacitance

R_{IG}: Resistance of intergranular boundary ($\rho \approx 10^{12}$ to 10^{13} Ω cm)

$R_{VAR:}$ Ideal varistor (0 to ∞ Ω)

$R_{B:}$ Bulk resistance of ZnO ($\rho \approx 1$ to 10 Ω cm)

Chapter 4 Simulation and Result

The software used in this simulation is ANSYS Simplorer. ANSYS Simplorer is a powerful platform for modeling, simulating and analyzing system-level digital prototypes. It has a unique ability to integrate high-fidelity models of power electronics.

The step of this simulation is:

(1) Built the IGBT model. The parameter of this model is according to the data sheet of Infineon FZ750R65KE3 IGBT.

(2) Built the MOV model. Using the non-linear resistor model to build MOV model using MOV V-I characteristic.

(3) Built the main circuit.

4.1Modeling

(1) IGBT modeling

(2) The parameter of this model is according to the data sheet of Infineon FZ750R65KE3 IGBT.

(3) Using characterize device to build the IGBT model.

(4) Choose basic dynamic IGBT model to build.

The input parameters of the dynamic IGBT model are nominal collector-emitter blocking voltage, nominal collector current, nominal reference temperature, leakage current, on-switch gate-emitter voltage, off-switch gate-emitter voltage, input capacitance, terminal chip resistance and stray inductance. These values can all be found from the datasheet. Then scan the Output characteristic (I_C = f (V_{CE}) V_{GE} = 15 V) Transfer characteristic (I_C = f (V_{GE}) V_{CE} = 20 V); Forward characteristic (I_F = f (V_F)) curves under nominal temperature and 25℃. All the curves can be found from the datasheet.

Built IGBT and diode thermal model. Determined the thermal circuit model and input the thermal resistance value such as IGBT thermal resistance junction to case, diode thermal resistance junction to case and thermal resistance case to heat sink.

Finally, input dynamic model parameters such as Ton Toff Eon Eoff.

The MOV model was built by a non linear resistor. We built it according its VI characteristic.

Simulation models were built for two different topologies. The first one is called module MOV topology and the second one is called one MOV topology.

The module MOV topology is shown as Figure 4-1. Each paralleled module was protected by a MOV. As there are six modules in series together, there are six MOVs protect these modules separately. The one MOV module only has a MOV to protect the whole modules, shown as Figure 4-2. These two different topologies may have different voltage stress and current stress. Analysis will be taken to compare the characteristic of these two topologies.

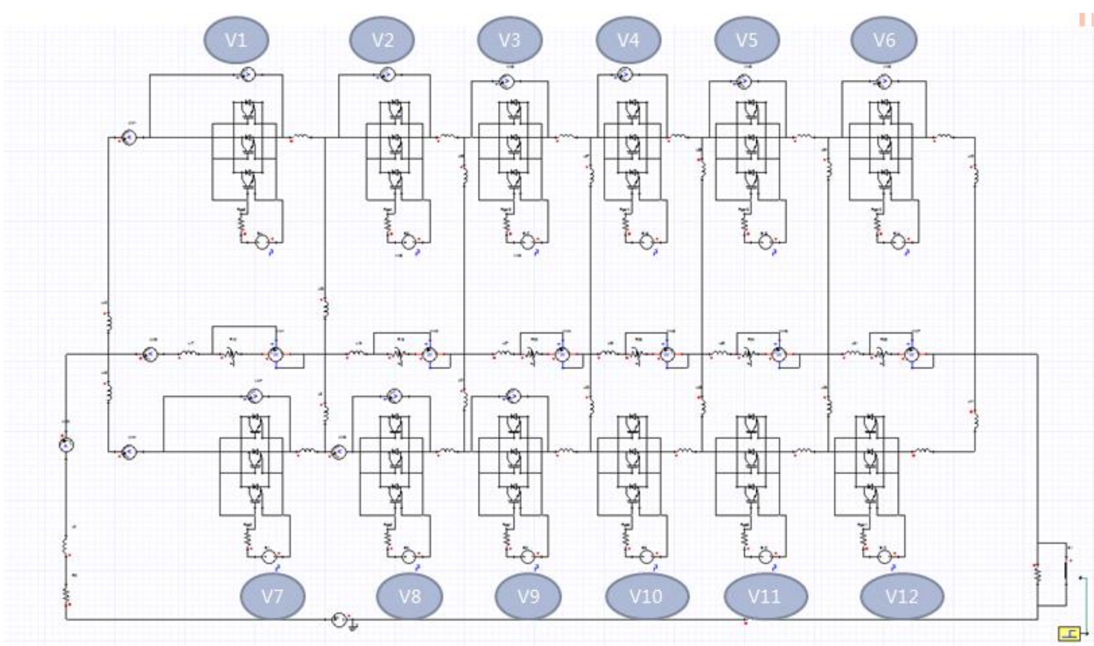

Figure 4-1 Module MOV mode simulation model

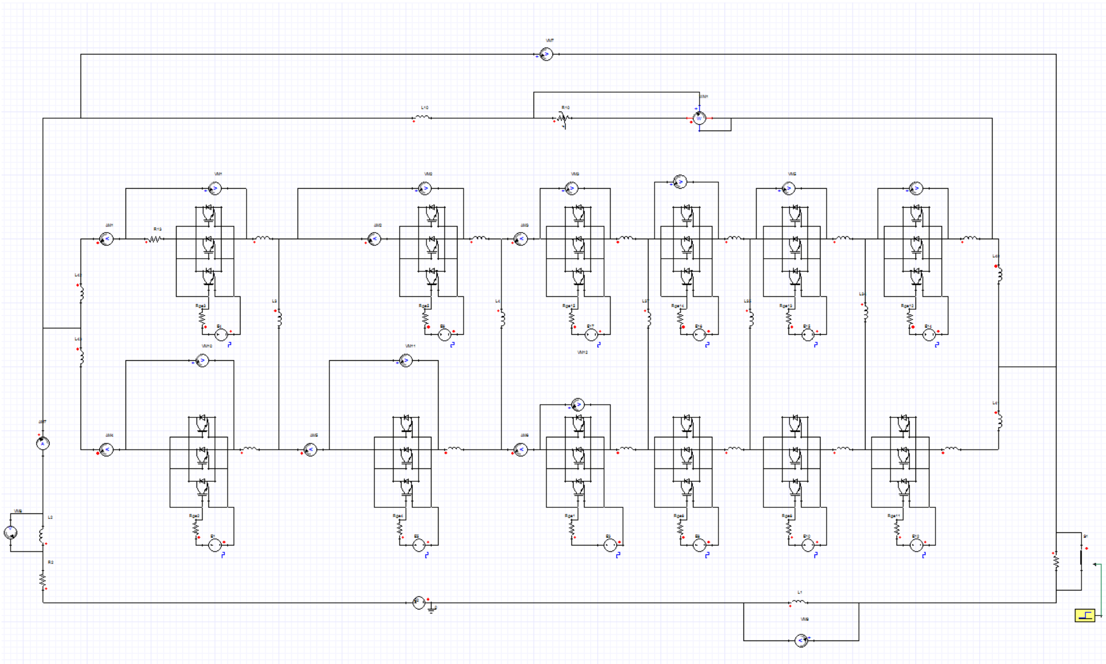

Figure 4-2

One MOV mode simulation model

4.2 Simulation model parameters

Table 5 to Table 8 show the simulation parameters in different situation.

Table 5 Module MOV mode fault occurs at 300m

Components	Values
DC source	20kV
Cable inductance	24.6μH
IGBT series stray inductance	18nH
IGBT parallel stray inductance	18nH
MOV stray inductance	50nH

Table 6 Module MOV mode fault occurs at 10m

Components	Values
DC source	20kV
Cable inductance	0.82μH
IGBT series stray inductance	18nH
IGBT parallel stray inductance	18nH
MOV stray inductance	50nH

Table 7 One MOV mode fault occurs at 300m

Components	Values
DC source	20kV
Cable inductance	24.6μH
IGBT series stray inductance	18nH

IGBT parallel stray inductance	18nH
MOV stray inductance	300nH

Table 8 One MOV mode fault occurs at 10m

Components	Values
DC source	20kV
Cable inductance	0.82μH
IGBT series stray inductance	18nH
IGBT parallel stray inductance	18nH
MOV stray inductance	300nH

4.3 Result and Analysis

4.3.1 Ideal condition

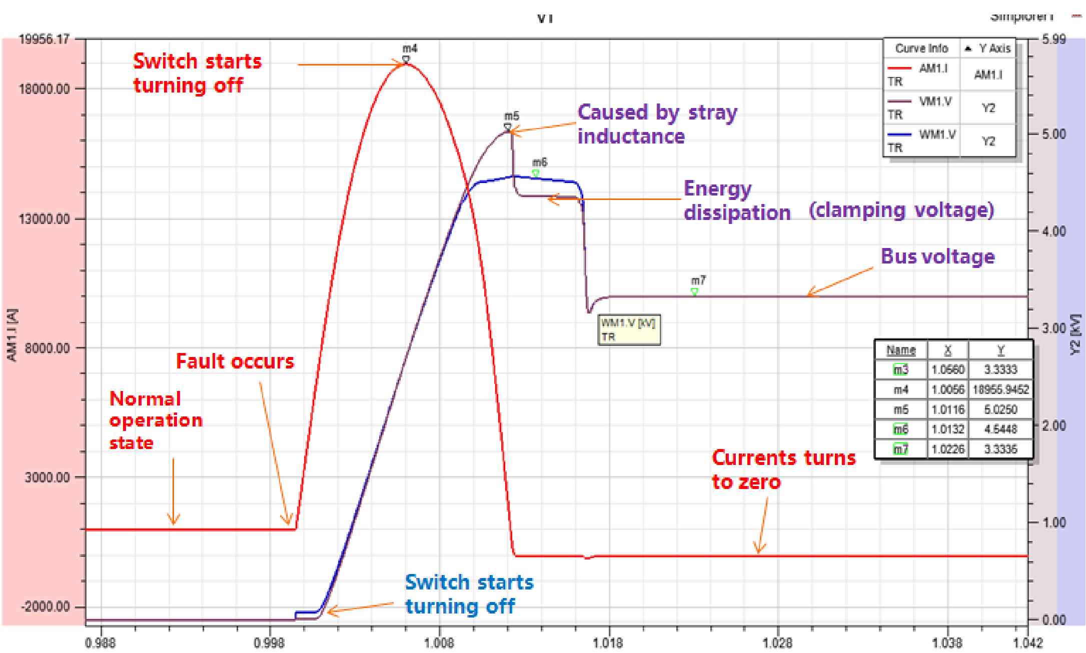

Figure 4-3 The current and voltage of an IGBT module and the voltage of MOV under Module MOV mode faults occurs at 10m

Figure 4-3 is module MOV mode faults occurs at 10m. The red line is the current curve of an IGBT module, the blue line is the voltage curve of an IGBT module and the purple line is the voltage curve of MOV. We can know from the current curve that at the beginning the circuit is under normal operation state. The current value is at the rating current value. It is 1000A. At 1ms, the system occurs a short circuits fault, the current starts to increase. The peak of the red curve is the maximum value of the fault current, and from then on, the switches start to turn off. After that the current starts to go down with the MOV dissipates the energy. Finally, the fault current turns to zero. We can know from the voltage curve of the IGBT module. First during the normal operation condition, the voltage value is only the conduction voltage drop, it is about several volts. At 1.02ms, that is 0.02ms after the fault occurs, the circuit breakers starts to turn off. Because the switches will not turn off instantaneously, so the voltage of the IGBT module will increase gradually. We all noticed that there is a voltage spike, the reason why there is a spike is that because the existing of stray inductance between MOV and IGBT modules. During that time the current changes rapidly, so the current change rate is really high which will generate a voltage. The voltage the IGBT needs to hold are the sum of the voltage which caused by the stray inductance, and the voltage which the MOV clamps. After a short time, the current change rate goes to zero, and the voltage spike disappears. After that the voltage between the IGBT is the voltage which the MOV clamps, after the energy dissipation of MOV the voltage goes back to the bus voltage. We can know from the voltage curve of the MOV, when there is no fault, MOV can be treated as a resistor which has a very large resistance value. When short circuit fault occurs and the IGBT stars to turn off, that is the voltage between MOV or IGBT starts to goes up, then the resistance value of MOV decreases rapidly and can be treated as a resistor which has a very small resistance value. Only in this way can MOV protect the IGBT. We can also notice that the voltage value of MOV is greater than the voltage between IGBT, this is because of the parallel and series stray inductance between IGBT and MOV.

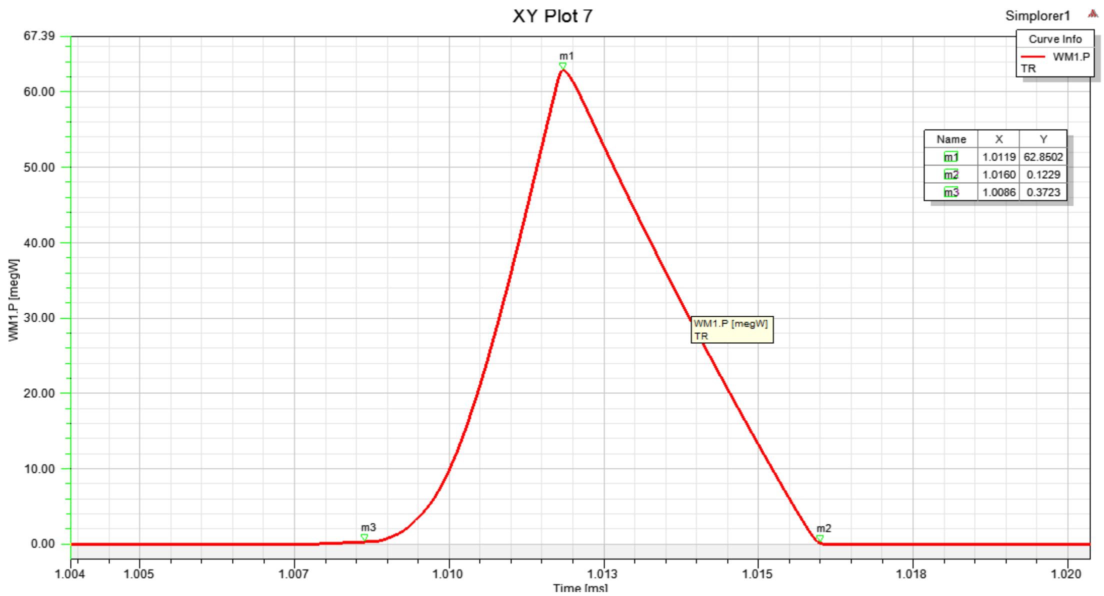

Fig Figure 4-4 The dissipation energy of MOV under Module MOV mode faults occurs at 10m under ideal condition

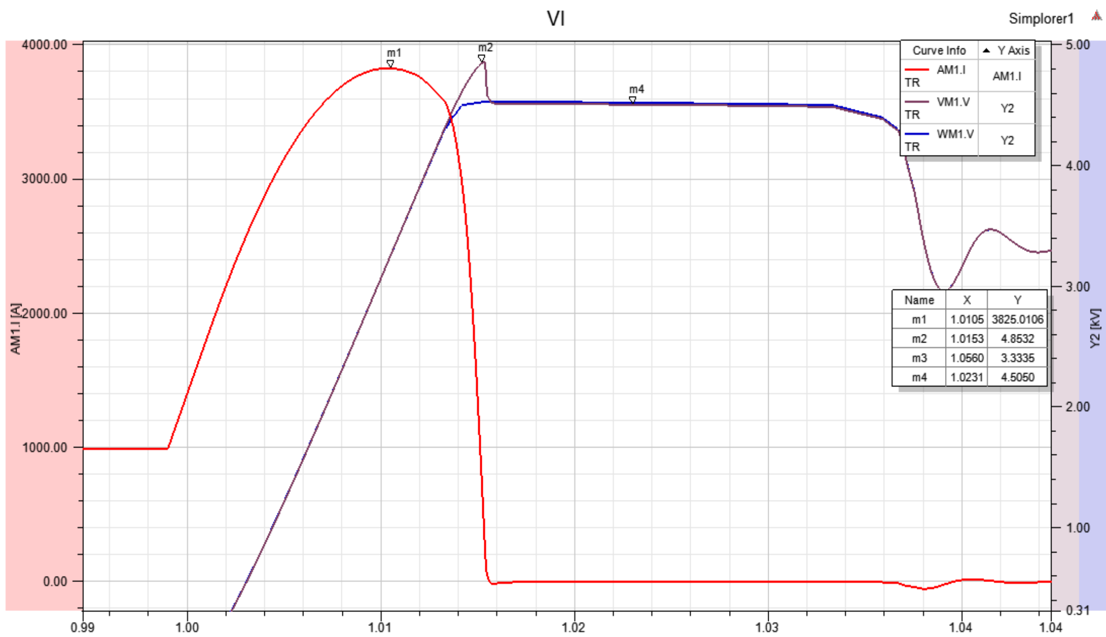

Figure 4-5 The current and voltage of an IGBT module and the voltage of MOV under module MOV mode faults occurs at 300m

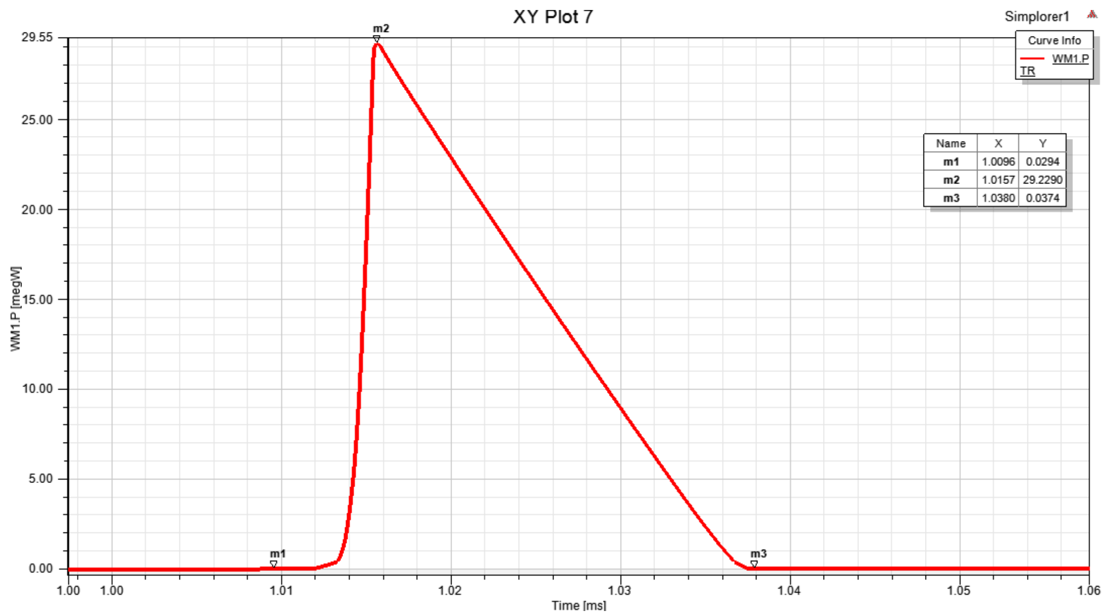

Figure 4-6 The dissipation energy of MOV under Module MOV mode faults occurs at 300m ideal condition

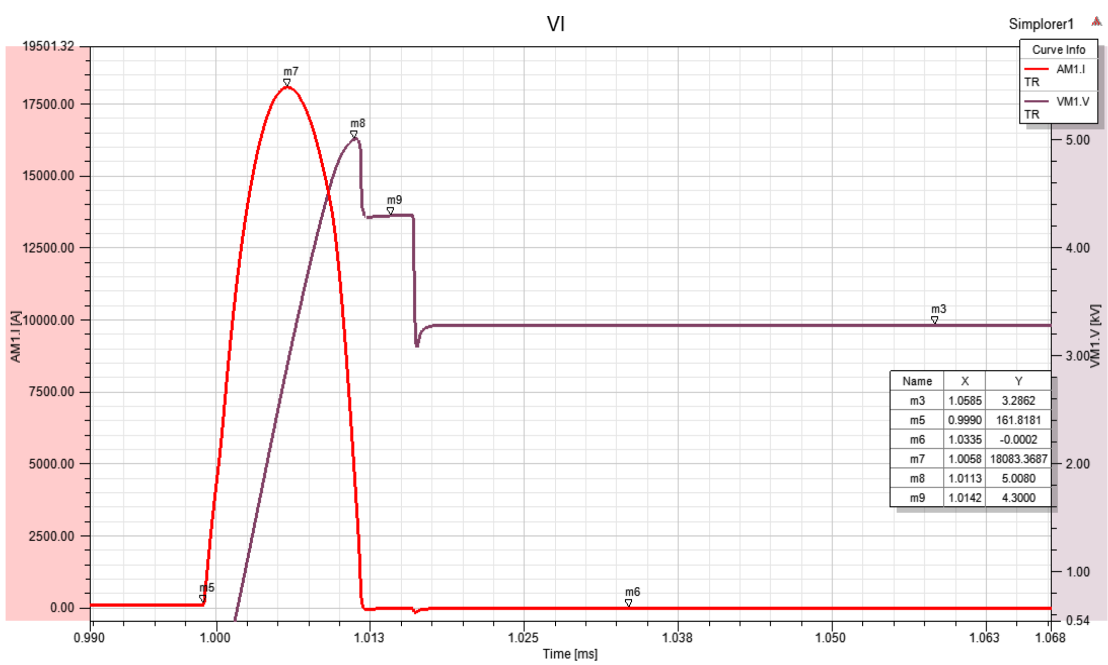

Figure 4-7 The current and voltage of an IGBT module and the voltage of MOV under one MOV mode faults occurs at 10m

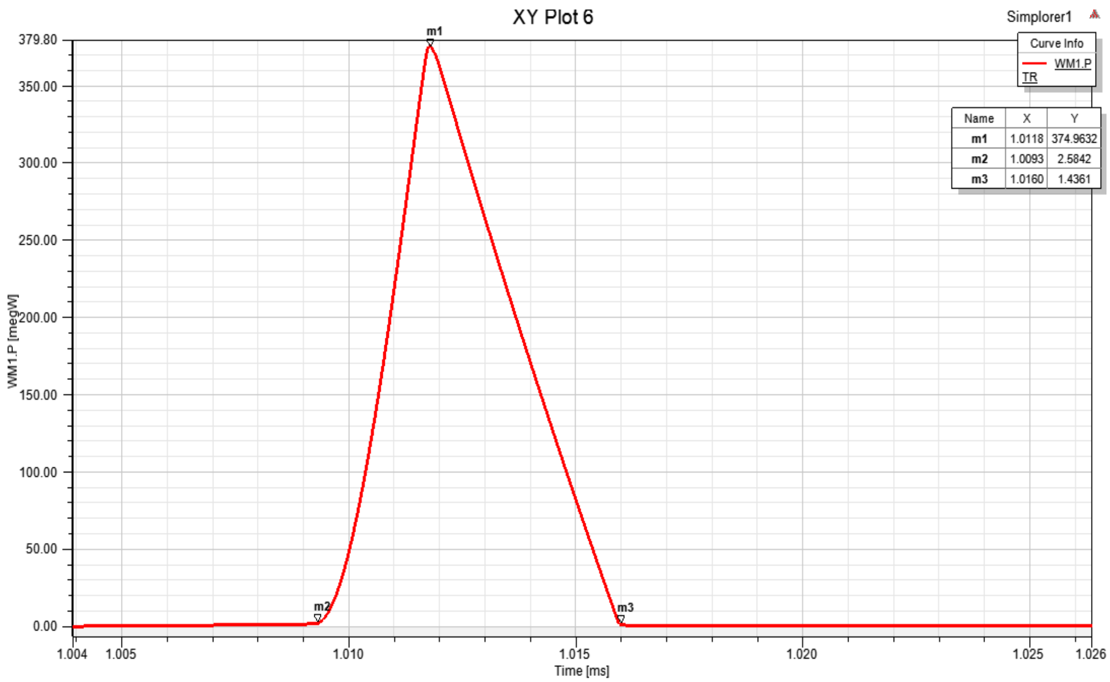

Figure 4-8 The dissipation energy of MOV under one MOV mode faults occurs at 10m ideal condition

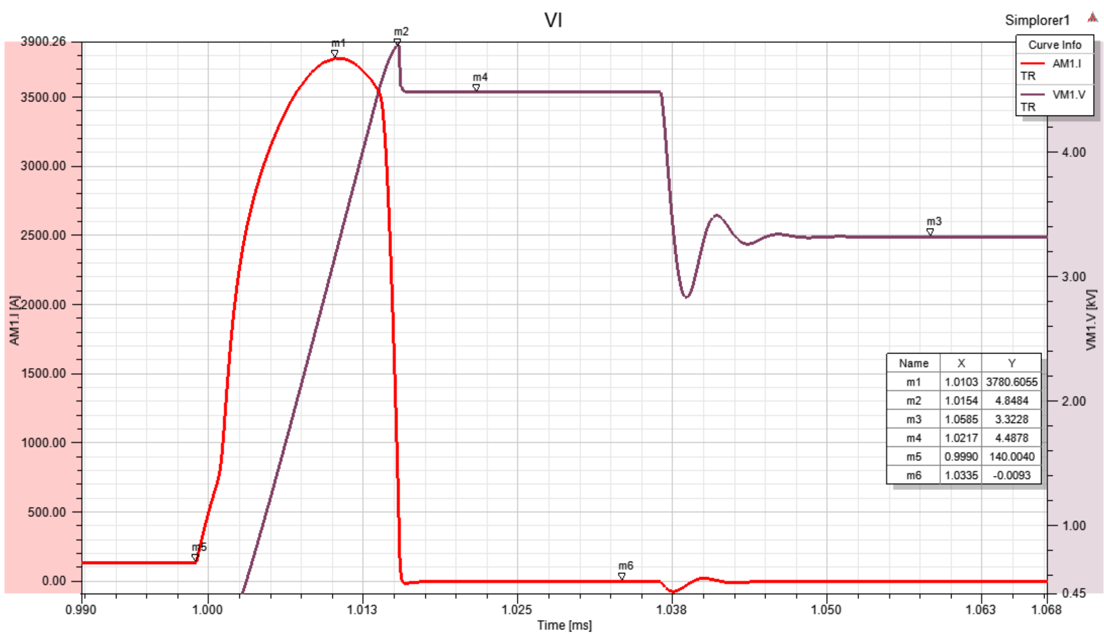

Figure 4-9 The current and voltage of an IGBT module and the voltage of MOV under one MOV mode faults occurs at 300m

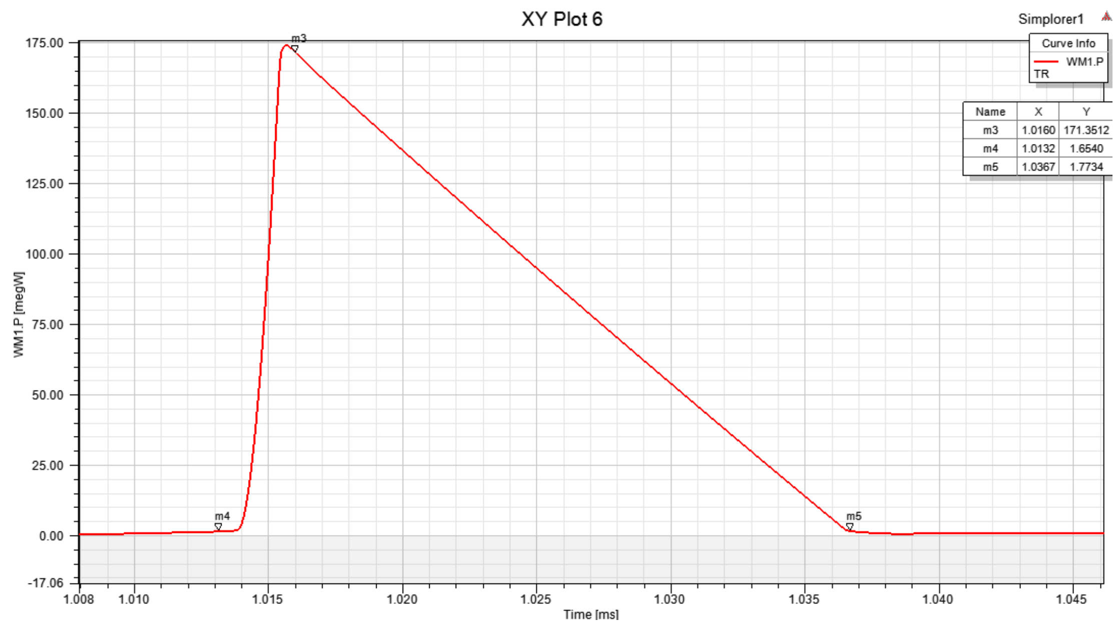

Figure 4-10 The dissipation energy of MOV under one MOV mode faults occurs at 10m ideal condition

Comparison of current and voltage stress of different mode

Table 9 different modes comparison

Comparison index \ mode	module MOV mode	one MOV mode
voltage stress/kV	4.8	4.85
current stress/A	3800	3816
energy dissipation/W	4350	4375

Under ideal condition, two modes are almost the same.

4.3.2Non-ideal condition

In the most of the time, the operation condition is not ideal. It may cause the voltage sharing and current sharing problems. In this part, four non-ideal conditions were simulated to simulate the factors which would cause current and voltage problems. The scenario simulated the dynamic sharing problem caused by the drive circuit: scenario 1 and scenario 2 and static sharing problem caused by parameter inconsistent: scenario 3 and scenario 4.

- Scenario 1: The gate signal of V1 is 2000ns earlier than others
- Scenario 2: The gate signal of V1 and V7 is 2000ns earlier than others
- Scenario 3: The resistance of V1 and V7 is 0.1mΩ greater than others
- Scenario 4: The resistance of V1 is 0.1mΩ greater than others

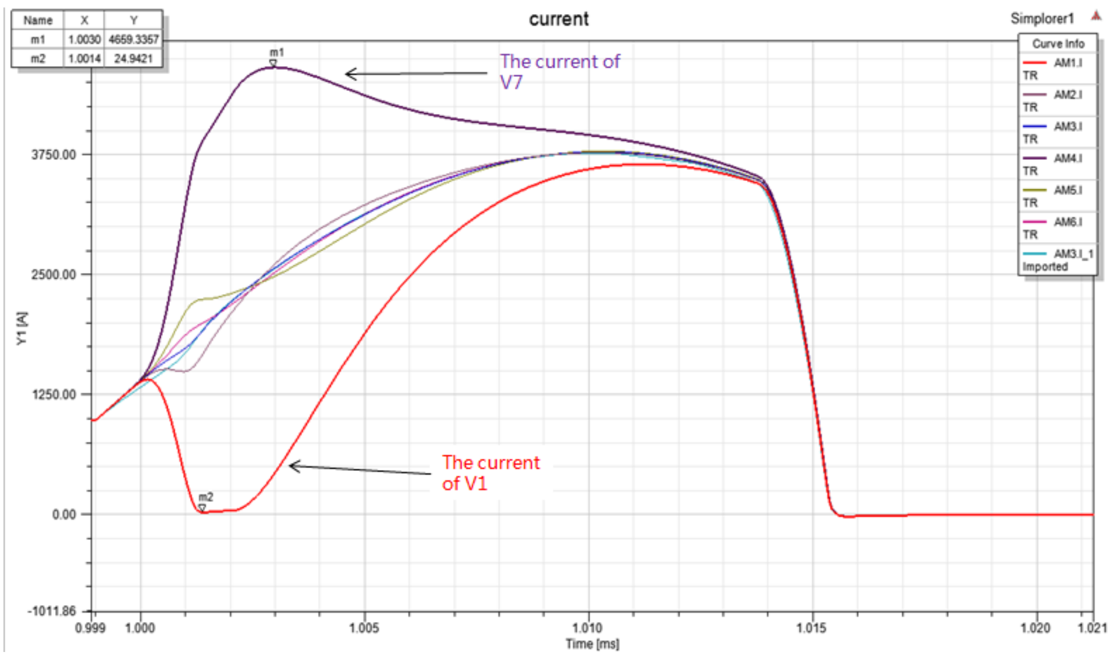

Figure 4-11 The gate signal of V1 is 2000ns earlier than others-current comparison of one MOV mode

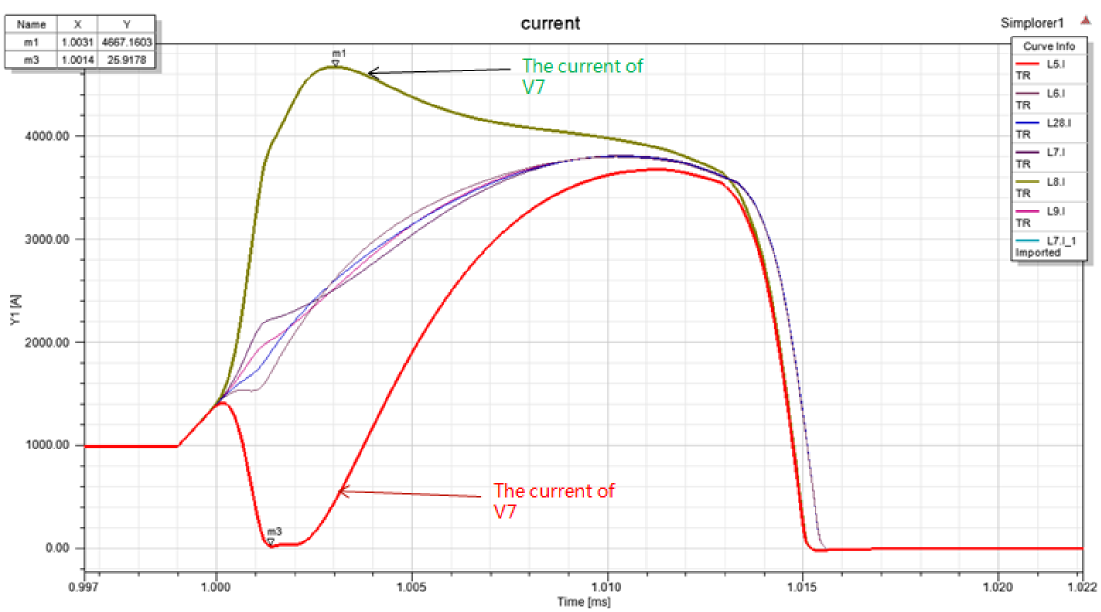

Figure 4-12 The gate signal of V1 is 2000ns earlier than others-current comparison of module MOV mode

From the two figures above, different gate signal in a parallel module may cause current sharing problem, the one which turns off earlier may have to carry a larger current.

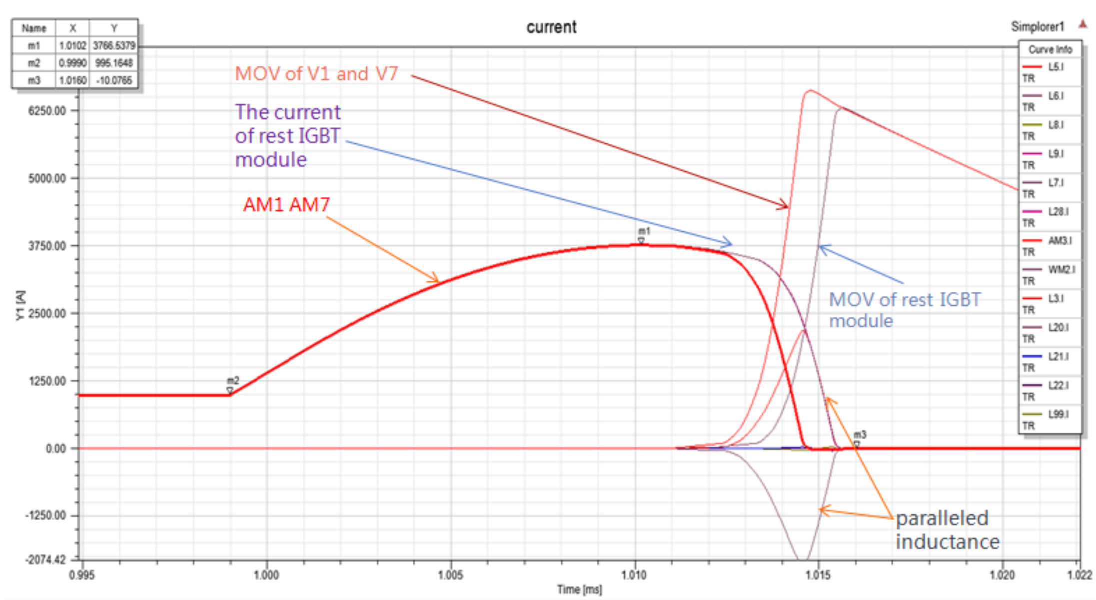

Figure 4-13 The gate signal of V1 is 2000ns earlier than others- currents through IGBT module MOV and paralleled inductance

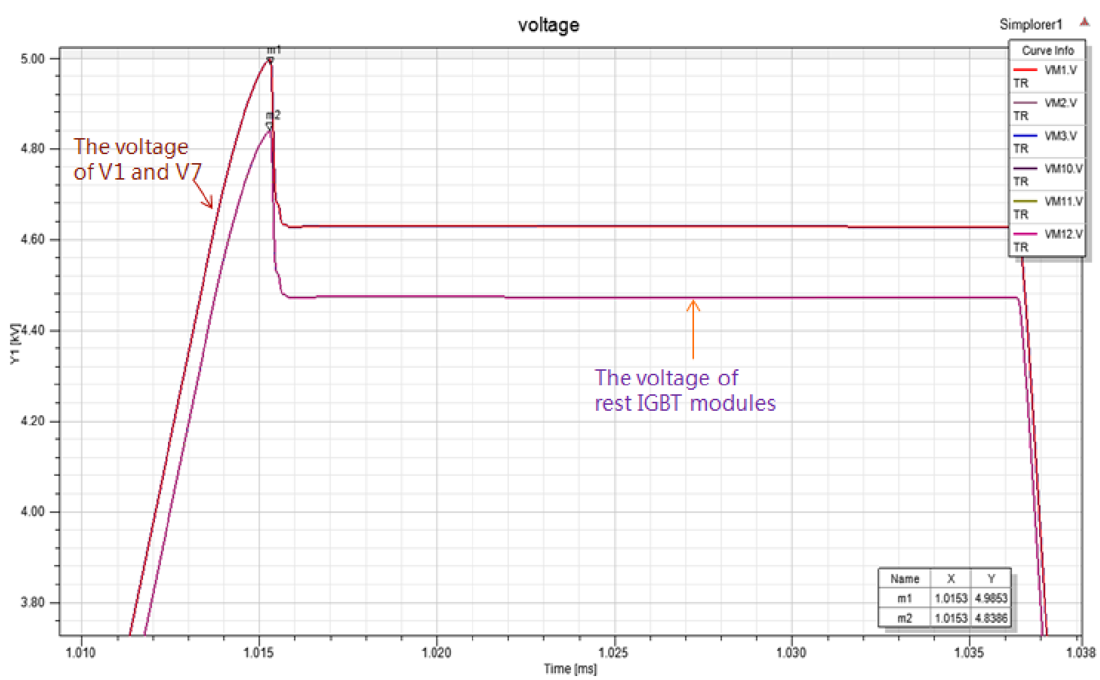

Figure 4-14 The gate signal of V1 is 2000ns earlier than others-voltage comparison of one MOV mode

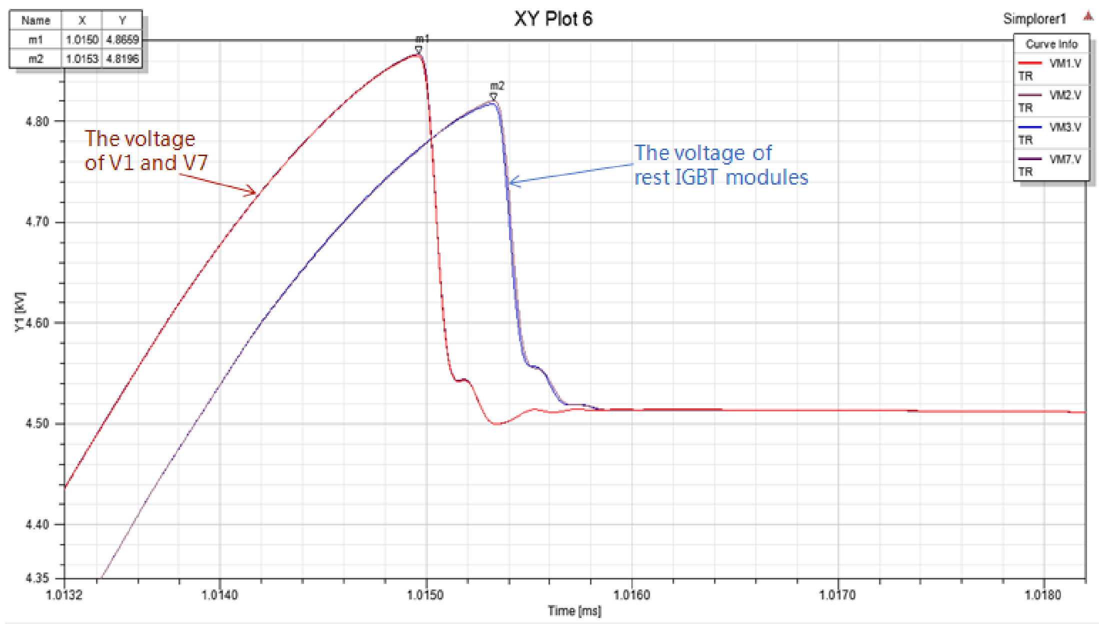

Figure 4-15 The gate signal of V1 is 2000ns earlier than others-voltage comparison of module MOV mode

From Fig and Fig, the parallel module no matter which drive signal is earlier than others no matter which branch turns off first, may need to hold a higher voltage. Compared with Fig and Fig, the one module mode have severe voltage stress.

Scenario 2

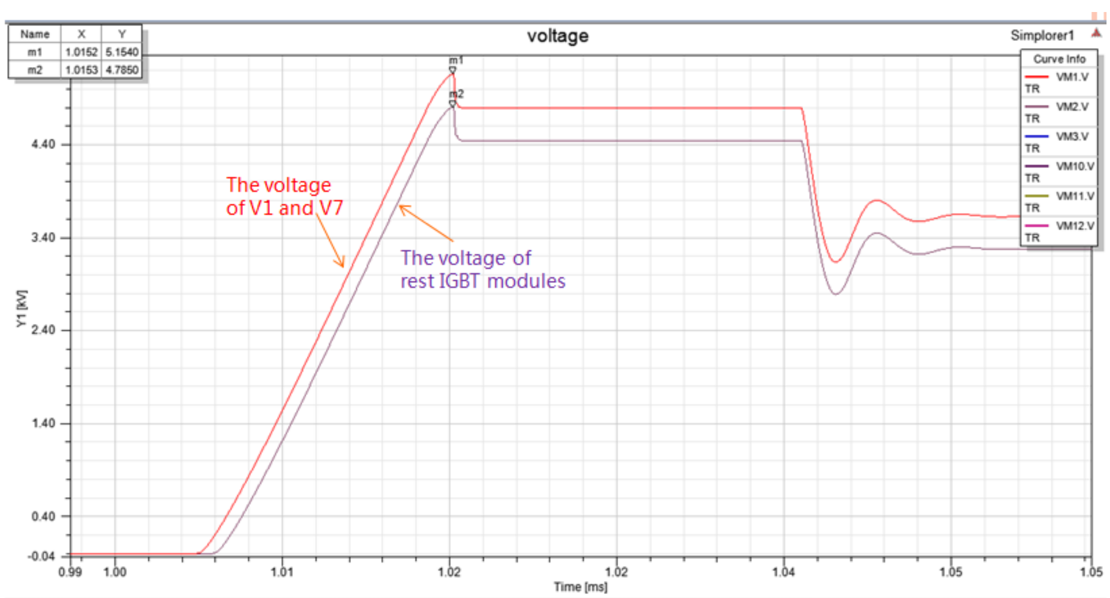

Figure 4-16 The gate signal of V1 and V7 is 2000ns earlier than others-voltage comparison of module MOV mode

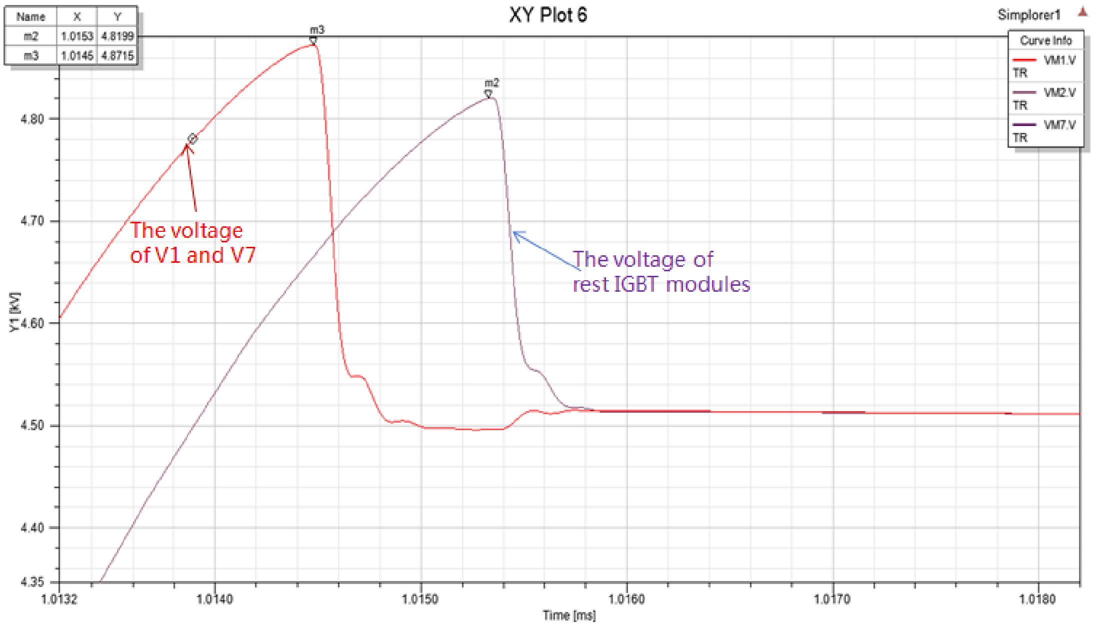

Figure 4-17 The gate signal of V1 and V7 is 2000ns earlier than others-voltage comparison of one MOV mode

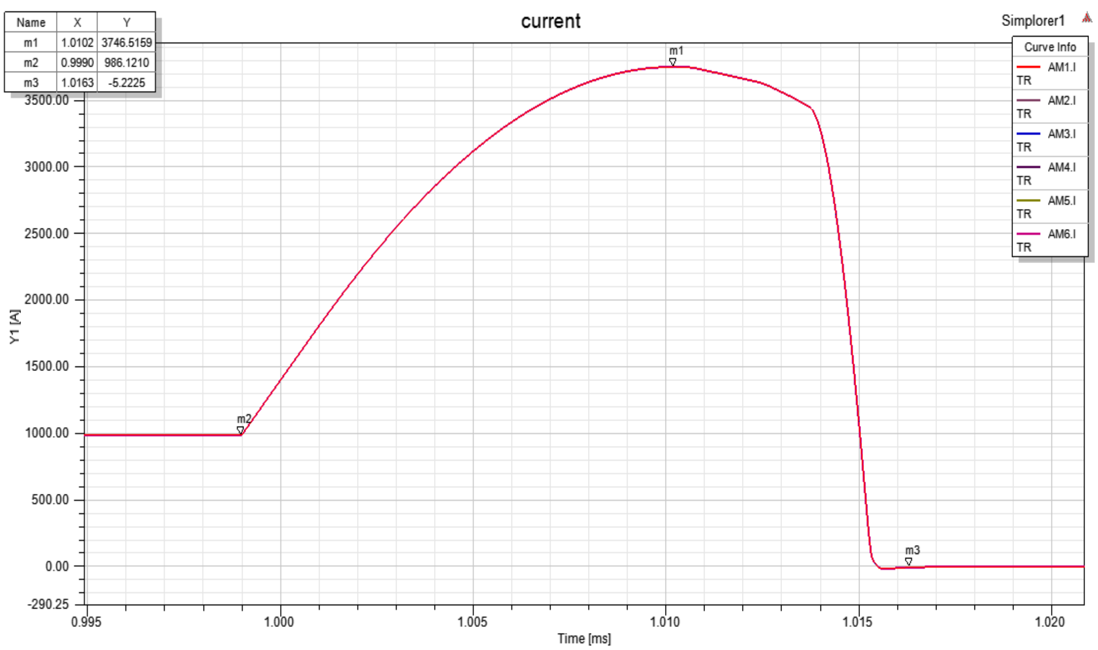

Figure 4-18 The gate signal of V1 and V7 is 2000ns earlier than others- current comparison of one MOV mode

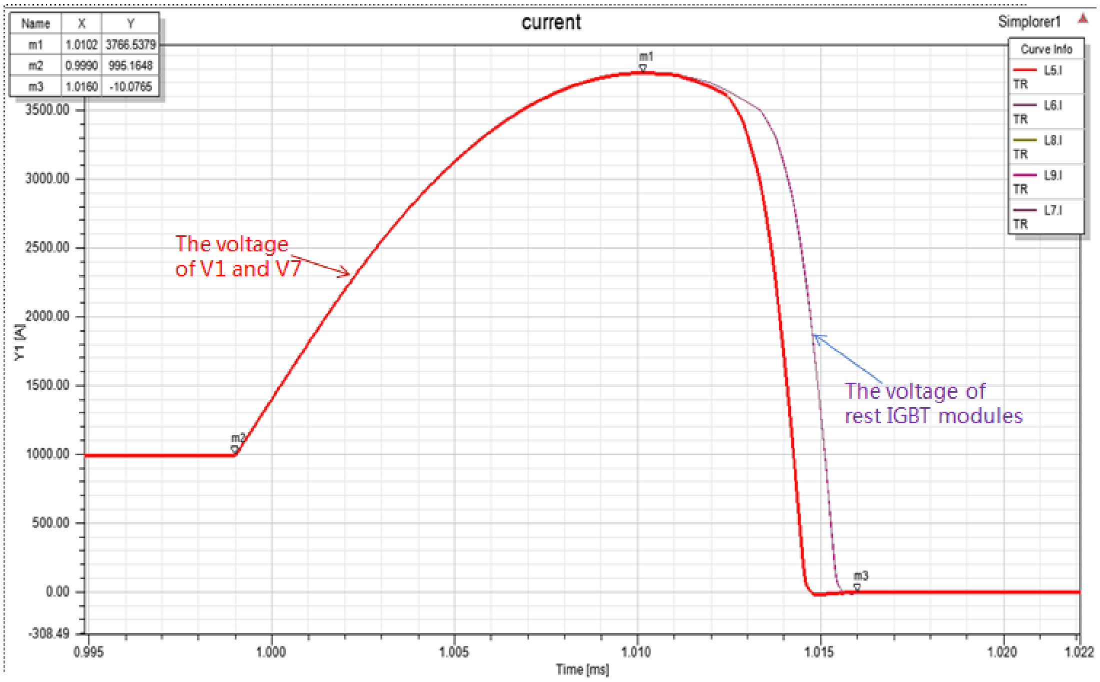

Figure 4-19 The gate signal of V1 and V7 is 2000ns earlier than others-current comparison of module MOV mode

Scenario 3

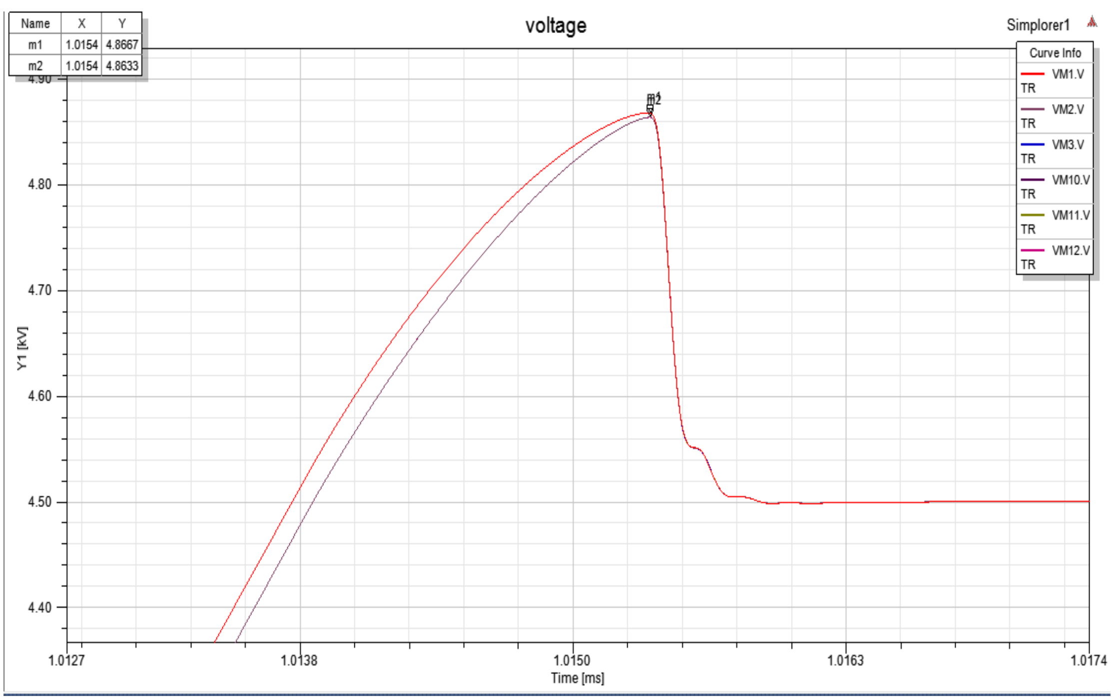

Figure 4-20 The resistance of V1 and V7 is 0.1mΩ greater than others-voltage comparison of one MOV mode

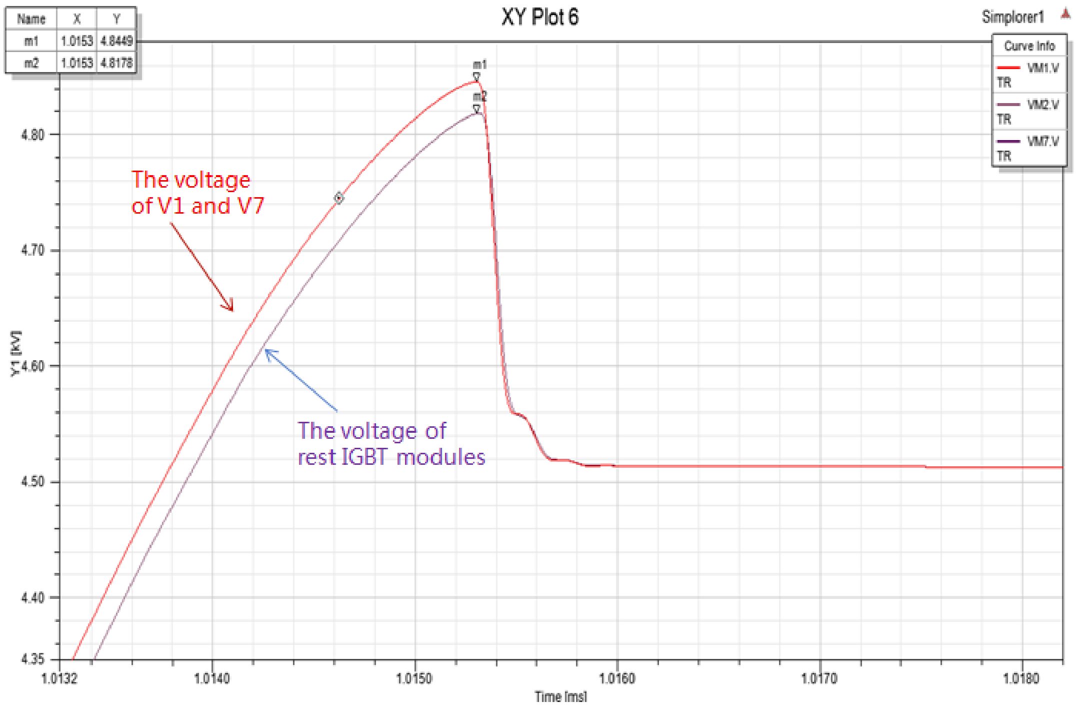

Figure 4-21 The resistance of V1 and V7 is 0.1mΩ greater than others-voltage comparison of module MOV mode

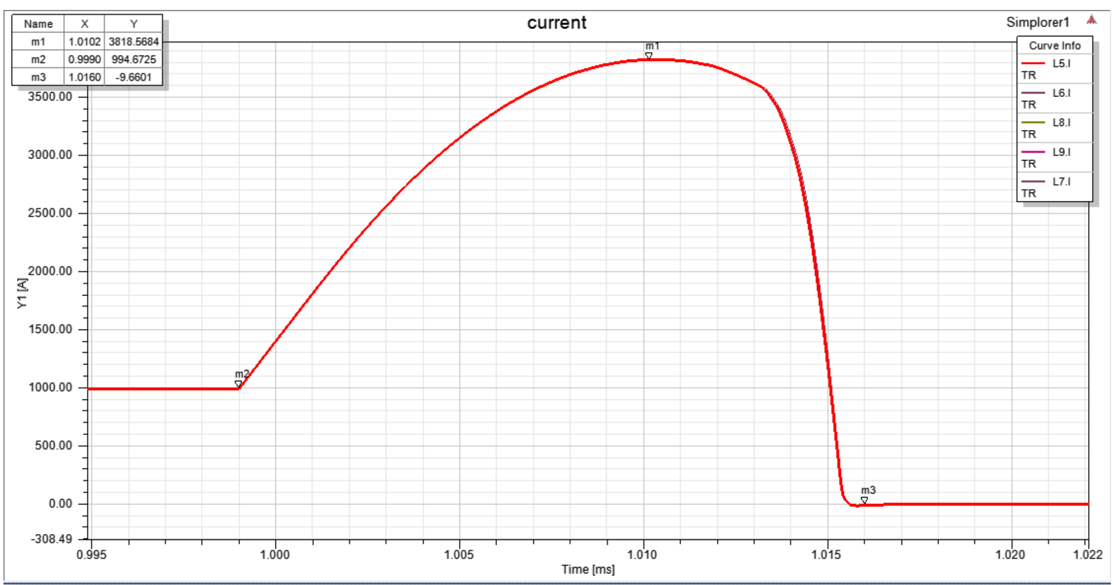

Figure 4-22 The resistance of V1 and V7 is 0.1mΩ greater than others-current comparison of module MOV mode

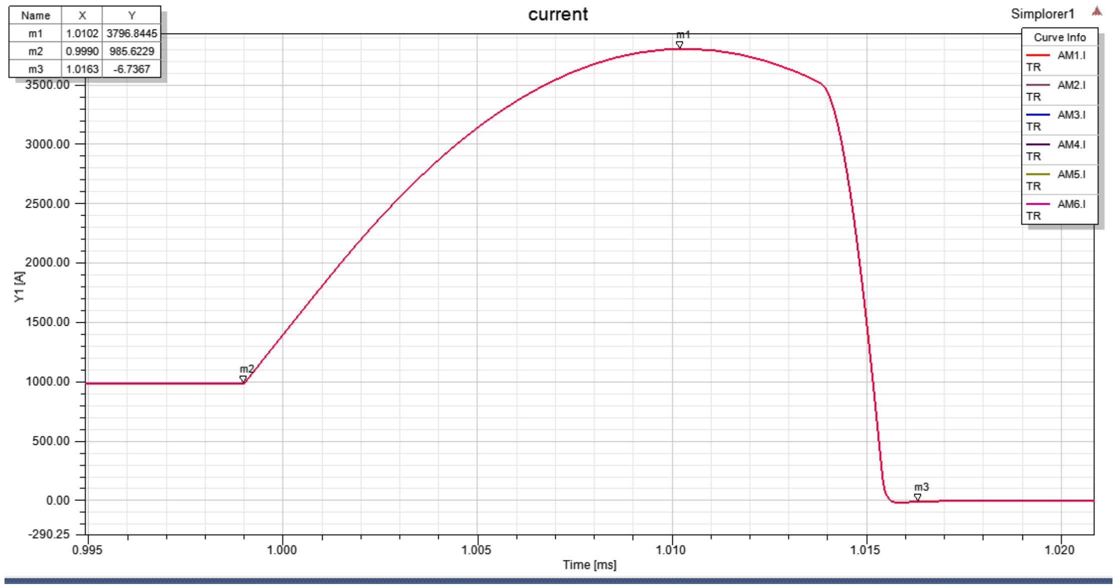

Figure 4-23 The resistance of V1 and V7 is 0.1mΩ greater than others-current comparison of one MOV mode

Scenario 4

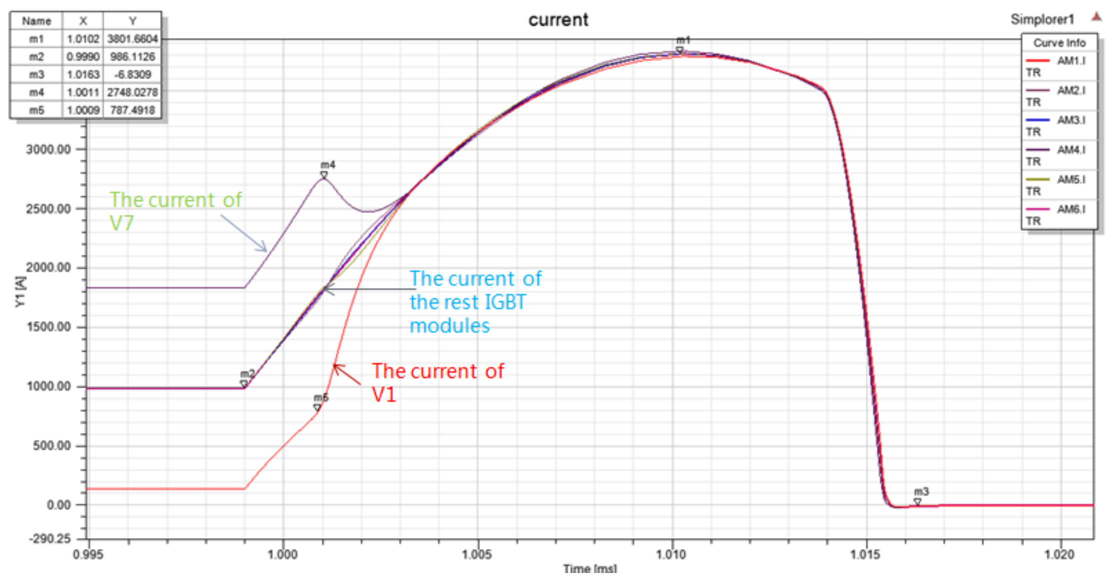

Figure 4-24 The resistance of V1 and V7 is 0.1mΩ greater than others- urrent comparison of one MOV mode

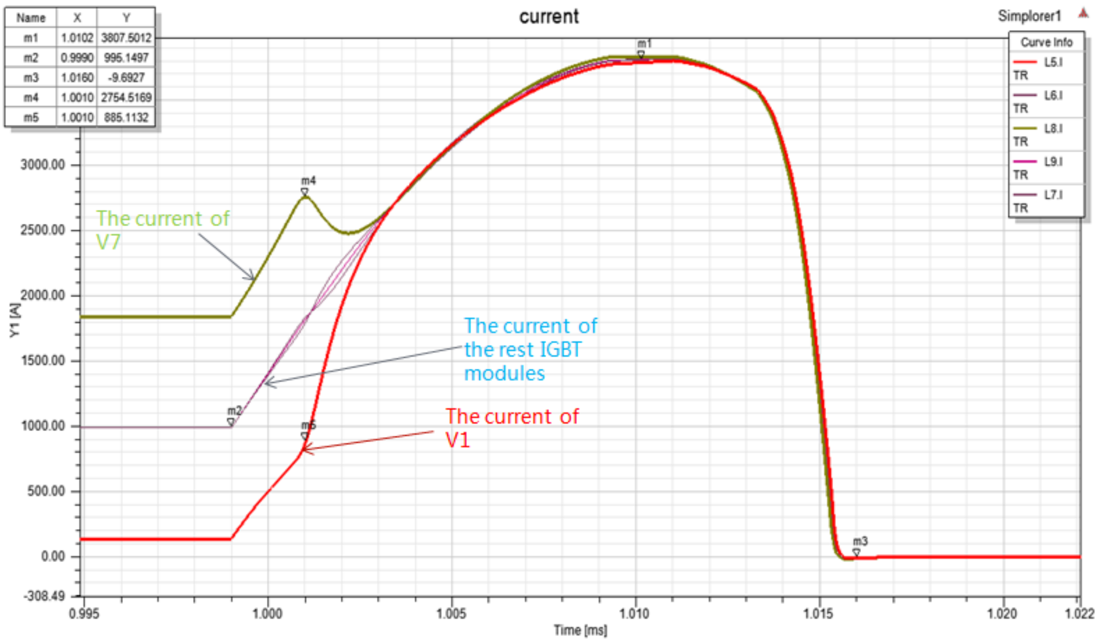

Figure 4-25 The resistance of V1 and V7 is 0.1mΩ greater than others-current comparison of module MOV mode

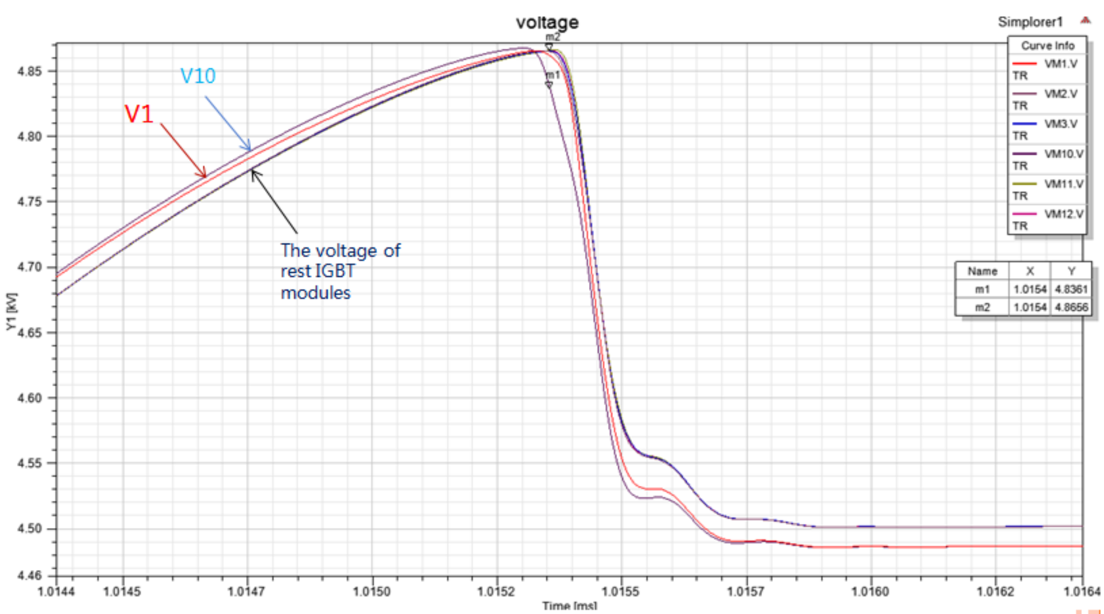

Figure 4-26 The resistance of V1 and V7 is 0.1mΩ greater than others-voltage comparison of one MOV mode

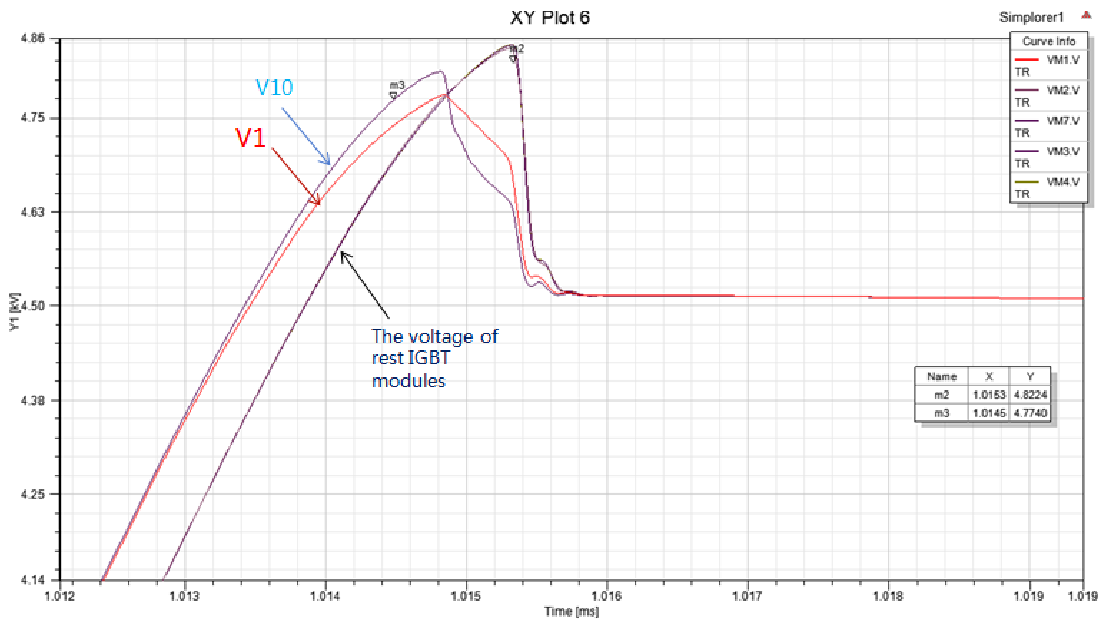

Figure 4-27 The resistance of V1 and V7 is 0.1mΩ greater than others-voltage comparison of module MOV mode

Chapter 5 Conclusion and Future Work

5.1 Conclusion

In the thesis, the thermal model of IGBT and diode has been compared. Then the thermal property of different kinds of semiconductor is analyzed to find the most suitable device for the medium voltage DC solid state circuit breaker and to find the maximum conduction current of the devices as well. A 6.5kV, 750A IGBT module from Infineon has been chosen for the proposed SSCB.

Next, two simulation models, one MOV model and module MOV model, are built in ANSYS to verify the previously analytical works. Based on the results of simulation, the conclusion of this thesis is that the module MOV mode is better than one MOV mode in achieving less voltage stress of semiconductors. One MOV mode suffers more severe unbalance voltage sharing. The connection of the devices should be more symmetrical to eliminate the impact of parallel stray inductance.

5.2 Future Work

First, the parasitic parameters which are the key elements in this design, need further discussion to get the accurate value of different mode.

Second, the calculation of thermal property for MOV should be taken into consideration in the future design to achieve a more precise thermal model.

References

[1] Madan, M. K., & Chowdhury, B. H. (2012, July). Solid state fault interruption devices in medium voltage microgrid distribution systems with distributed energy resources. In *Power and Energy Society General Meeting, 2012 IEEE* (pp. 1-6). IEEE

[2] Shen, Z. J., Sabui, G., Miao, Z., & Shuai, Z. (2015). Wide-bandgap solid-state circuit breakers for DC power systems: Device and circuit considerations. *IEEE Transactions on Electron Devices, 62*(2), 294-300.

[3] Magnusson, J. (2015). *On the design of hybrid dc-breakers consisting of a mechanical switch and semiconductor devices* (Doctoral dissertation, KTH Royal Institute of Technology).

[4] E. O. Norum, "Protection system for dc grid applications," Dec 2014, specialization project,NTNU.

[5] WG.B4.52, "Hvdc grid feasibility study," CIGRE, Technical Brochure, Apr 2013.

[6] Norum, E. Ø. (2016). *Design and Operation Principles of DC Circuit Breakers-Development of a Solid State DC Breaker for the NTNU/SINTEF Smart Grid and Renewable Energy Laboratory* (Master's thesis, NTNU).

[7] E. O. Norum, "Protection system for dc grid applications," Dec 2014, specialization project, NTNU.

[8] Shammas, N. Y. A., Withanage, R., & Chamund, D. (2006). Review of series and parallel connection of IGBTs. *IEE Proceedings-Circuits, Devices and Systems, 153*(1), 34-39.

[9] Nakatake, H., & Iwata, A. (2003, June). Series connection of IGBTs used multilevel clamp circuit and turn off timing adjustment circuit. In *Power Electronics Specialist Conference, 2003. PESC'03. 2003 IEEE 34th Annual* (Vol. 4, pp. 1910-1915). IEEE.

[10] Raciti, A., Belverde, G., Galluzzo, A., Greco, G., Melito, M., & Musumeci, S. (2001). Control of the switching transients of IGBT series strings by high-performance drive units. *IEEE Transactions on Industrial Electronics, 48*(3), 482-490.

[11] Hofer, P., Karrer, N., & Gerster, C. (1996, June). Paralleling intelligent IGBT power modules with active gate-controlled current balancing. In *Power Electronics Specialists Conference, 1996. PESC'96 Record., 27th Annual IEEE* (Vol. 2, pp. 1312-1316). IEEE.

[12] Baek, J. W., Yoo, D. W., & Kim, H. G. (2001). High-voltage switch using series-connected IGBTs with simple auxiliary circuit. *IEEE Transactions on Industry Applications, 37*(6), 1832-1839.

[13] Schnell, R., Bayer, M., & Geissmann, S. (2011). Thermal design and temperature ratings of IGBT modules. *ABB, Switzerland, available at: http://www05. abb. com/global/scot/scot256.nsf/veritydisplay/754216faaa21d0e6c125791f0046de68/$ file/5SYA.*

[14] Rohner, S., Bernet, S., Hiller, M., & Sommer, R. (2010). Modulation, losses, and semiconductor requirements of modular multilevel converters. *IEEE transactions on Industrial Electronics*, *57*(8), 2633-2642.

[15] LYTRON. Product Datasheet [Online]. Available: http://www.lytron.com/Tools-and-Technical-Reference/Application-Notes/Selecting-A-Cold-Plate-Technology.

[16] Birk, J., & Andresen, B. (2007, September). Parallel-connected converters for optimizing efficiency, reliability and grid harmonics in a wind turbine. In *Power Electronics and Applications, 2007 European Conference on* (pp. 1-7). IEEE.

[17] Infineon. Product Datasheet [Online]. Available: http://www.infineon.com/dgdl/Infineon-FZ600R65KE3-DS-v03_00-EN.pdf?fileId=db3a30432c64a60d012cbbecaa6f0356

[18] Infineon. Product Datasheet [Online]. Available: http://www.infineon.com/dgdl/Infineon-FZ750R65KE3-DS-v03_01-EN.pdf?fileId=db3a304325afd6e00126461fd3936974.

[19] ABB Switzerland Ltd. Product Datasheet [Online]. Available: https://library.e.abb.com/public/d2906e423b0244b6b3566e4b72f30d39/5SNA%200600G650100_5SYA%201558-05%2011-2015.pdf.

[20] ABB Switzerland Ltd. Product Datasheet [Online]. Available: https://library.e.abb.com/public/b47d6dffcf024d33a38f4f2bb2ed1896/5SNA%200750G650300_5SYA%201600-04%2003-2016.pdf.

[21] ABB Switzerland Ltd. Product Datasheet [Online]. Available: https://library.e.abb.com/public/500afc0e0e6f00dcc125776200506d71/5STF_11F3010.pdf.

[22] ABB Switzerland Ltd. Product Datasheet [Online]. Available: https://library.e.abb.com/public/2bc16f97ef5ee0d5c1257913004c60eb/5STF_06T2440.pdf.

[23] ABB Switzerland Ltd. Product Datasheet [Online]. Available: https://library.e.abb.com/public/8d6eb6e4faf52ba6c1257641002a1019/5SGA%2006D4502_5SYA1236-00.pdf

[24] Wen, Y., Yan, X., Yi, X., & Zhou, C. (2004). Investigation into the equivalent circuit of MOV and the determination of its parameters. *IEEE Transactions on Power Delivery*, *19*(3), 1091-1094.

[25] Li, H. S., & Tan, J. C. (2014, September). New Algorithm for On-state Loss of Thyristor Valve. In *Electricity Distribution (CICED), 2014 China International Conference on* (pp. 584-586). IEEE.

[26] EPCOS, A. (2011). General technical information. *SIOV metal oxide varistors*.

[27] Magnusson, J., Saers, R., Liljestrand, L., & Engdahl, G. (2014). Separation of the energy absorption and overvoltage protection in solid-state breakers by the use of parallel varistors. *IEEE transactions on power electronics*, *29*(6), 2715-2722.

[28] .Patil, K., & Grande-Moran, C. (2012). Modeling Metal Oxide Varistors (MOV) in Short Circuit Calculations. *SIEMENS–Power Technology*, (111), 1-6.

[29] Magnusson, J., Bissal, A., Engdahl, G., & Martinez-Velasco, J. A. (2014, October). Design aspects of a medium voltage hybrid DC breaker. In *Innovative Smart Grid Technologies Conference Europe (ISGT-Europe), 2014 IEEE PES* (pp. 1-6). IEEE.

[30] Singh, V. (2016). *Solid state protective device topological trade-offs for MVDC systems* (Doctoral dissertation, The University of Wisconsin-Milwaukee).